Dynamics of eddy-driven North Atlantic Oscillations in a localized shifting jet: zonal structure and downstream blocking

Dehai Luo · Wen Zhou · Ke Wei

Abstract In a weakly nonlinear model how an initial dipole mode develops to the North Atlantic Oscillation (NAO) in a localized shifting jet under the prescribed eddy forcing is examined. It is found that the zonal structure of the eddy-driven NAO anomaly is not only dominated by the longitudinal distribution of the preexisting Atlantic storm track, but also by the initial condition of the NAO anomaly itself associated with the interaction between a localized shifting jet and a topographic standing wave over the Atlantic basin. When both the initial NAO anomaly and the eddy vorticity forcing in the prior Atlantic storm track are more zonally localized, the subsequent eddy-driven NAO anomaly can be more zonally isolated and asymmetric. But, it seems that the shape of the initial NAO anomaly associated with the latitudinal shift of a prior Atlantic jet plays a more important role in producing the zonal asymmetry of subsequent NAO patterns. The zonal asymmetry of the NAO anomaly can be enhanced as the height of topography increases. In addition, it is further found that blocking events occur easily over the Europe continent through the decaying of positive-phase NAO events. However, prior to the positive-phase NAO life cycle the variability in each of three factors: the Atlantic jet, the eddy vorticity forcing in the Atlantic storm track and the initial NAO anomaly can result in a variation in the blocking activity over the Europe sector in strength, duration, position and pattern.

1 Introduction

The North Atlantic Oscillation (NAO) is an important low-frequency dipole mode of atmospheric variability in the northern hemisphere (NH), linked to a change in local and global climates (Hurrell 1995; Wallace 2000). Albeit the stratosphere and the ocean can influence the NAO on decadal timescales, the NAO with short timescales of several weeks has been found to be essentially originated from the internal dynamics of atmospheric motions, i.e., the forcing of synoptic-scale eddies in the Atlantic storm track (Feldstein 2003; Benedict et al. 2004).

Observation and numerical experiments show that observed NAO patterns are zonally isolated and asymmetric (Wallace 2000; Cash et al. 2002, 2005; Vallis et al. 2004; Gerber and Vallis 2005; Feldstein and Franzke 2006), and concluded to be probably tied to the variability of the Atlantic storm track (Löptien and Ruprecht 2005; Vallis and Gerber 2008) and to the stationary wave forcing (DeWeaver and Nigam 2000; Cash et al. 2002, 2005). Vallis et al. (2004) found that the resulting dipole mode can be zonally isolated and is similar to the NAO pattern, if the stirring forcing provided by the Atlantic storm track is confined in a zonally localized region. Cash et al. (2005) noted in a GCM that there is a strong positive link between the strength of the EOF asymmetries of annular modes and the strength of the storm track localization, and the zonal asymmetry of the annular mode is enhanced as the zonally

D. Luo (✉)
College of Physical and Environmental Oceanography,
Ocean University of China, 266003 Qingdao, China
e-mail: ldh@ouc.edu.cn

D. Luo · W. Zhou · K. Wei
CityU-IAP Laboratory for Atmospheric Sciences,
Department of Physics and Material Sciences,
City University of Hong Kong, Hong Kong, China

K. Wei
Center for Monsoon System Research, IAP,
Chinese Academy of Science, Beijing, China

asymmetric boundary conditions including a Gaussian mountain similar to the Tibetan Plateau are included. However, how the zonal asymmetry of the NAO anomaly depends upon the parameters is not completely clear. In particular, what factors affect the zonal structure of the eddy-driven NAO is not investigated in detail in previous studies. Recently, it has been indicated that the occurrence of the NAO is a nonlinear initial-value problem (Benedict et al. 2004; Franzke et al. 2004). Thus, this motivates us to conjecture that the zonal structure of eddy-driven NAO anomalies may be dominated by the initial structures of planetary- and synoptic-scale waves associated with the NAO life cycle, which is evidently different from previous studies.

More recently, a precise relationship between the wave breaking, the latitudinal shift of westerly jet and the NAO occurrence has been widely discussed by Luo et al. (2007b, 2008a) in a weakly nonlinear analytical model. The major advantage of the analytical approach can shed light on the physical dynamics of the eddy-driven NAO life cycle. In particular, Luo et al. (2008b) found that the north–south shift of the Atlantic jet prior to the NAO tends to control the phase of subsequent NAO events. However, the zonal structure of the NAO anomaly and its link with the longitudinal distribution of the Atlantic storm track, the initial value of the NAO anomaly and a localized shifting jet are not examined in these studies. Observations indicate that the midlatitude jet prior to the NAO are more likely to exhibit a localized variability (Lee and Kim 2003; Eichelberger and Hartmann 2007), it is, thus, natural that the weakly nonlinear NAO model proposed in Luo et al. (2008b) should be extended to include a background jet with a local variability in both position and strength to investigate the zonal structure of eddy-driven NAO anomalies in a localized shifting jet.

On the other hand, observations also show that there is a positive correlation between the NAO and blocking events over the European continent. Statistically, the positive phase of the NAO tends to favor the occurrence of blocking events over the European continent (Scherrer et al. 2006). However, there is not a one-to-one correspondence between the positive phase NAO event and the European blocking event (Luo et al. 2007a). Thus, it is concluded that other factors can, to some extent, influence the occurrence of European blocking events during the life cycle of positive-phase NAO events.

In this paper, we will find that except for the effect of the longitudinal distribution of preexisting synoptic-scale eddies noted in Vallis et al. (2004) the initial value of the NAO anomaly and the topographic height can also affect the zonal structure of the NAO anomaly. In addition, we will also investigate what factors affect the blocking activity over the European continent during the life cycles

of positive phase NAO events by using a generalized weakly nonlinear NAO model.

This paper is organized as follows: In Sect. 2 we present the time-latitude evolution of vertical and zonal mean zonal winds over the Atlantic and Pacific basins based on a composite of NAO events for each phase of NAO to see the difference of the prior Atlantic jet between two phases of NAO. In Sect. 3, we use a linearized equivalent barotropic model to demonstrate how an initial isolated dipole mode is excited and how it is connected to the localized shift of a jet in position. In Sect. 4, the weakly nonlinear NAO model established by Luo et al. (2007a, b, 2008a, b) is extended to include a localized shifting jet. The zonal structure of the eddy-driven NAO anomaly and its link with the initial value of the NAO anomaly and the longitudinal distribution of a preexisting storm track are examined in Sect. 5. In Sect. 6, we will focus on discussing what factors affect the occurrence of European blocking events associated with positive phase NAO events. Section 7 is devoted to discuss the local variability of the westerly jet during the NAO life cycle and its relation with the zonal structure of the NAO anomaly. Conclusion and discussions are summarized in Sect. 8.

2 Regional variability of observed jets during the NAO life cycle

Figure 1 shows the time-latitude evolution of vertical (from 1,000 to 300 hPa) and zonal mean zonal winds over the Atlantic and Pacific basins in terms of a composite of NAO events for two phases of the NAO based on the daily NAO indices given by Benedict et al. (2004). It is found that although the variation in jet position is most prominent at the mature stage (Lag 0) of the NAO life cycle, during the pre-period of this NAO life cycle (from −Lag 30 to −Lag 10) the difference of the jet position between the positive and negative phases is also distinct over the Atlantic sector. In other words, prior to the NAO the jet position is more north for the positive phase than for the negative phase. Thus, the north–south variability of the westerly jet prior to the NAO is a precursor of whether the NAO is positive or negative (Luo et al. 2008b). However, what processes drive the local variability of the westerly jet prior to the NAO life cycle is unclear and its further investigation is beyond the scope of this paper. At the same time, we can see that over the Pacific sector the variability in jet position between two phases of NAO is less distinct compared to that over the Atlantic basin. This suggests that the variability of the prior Atlantic jet in position be zonally localized. Because a meridional shift of the westerly jet that is uniform in the zonal direction is only considered in Luo et al. (2008b), their weakly nonlinear NAO model is inappropriate for
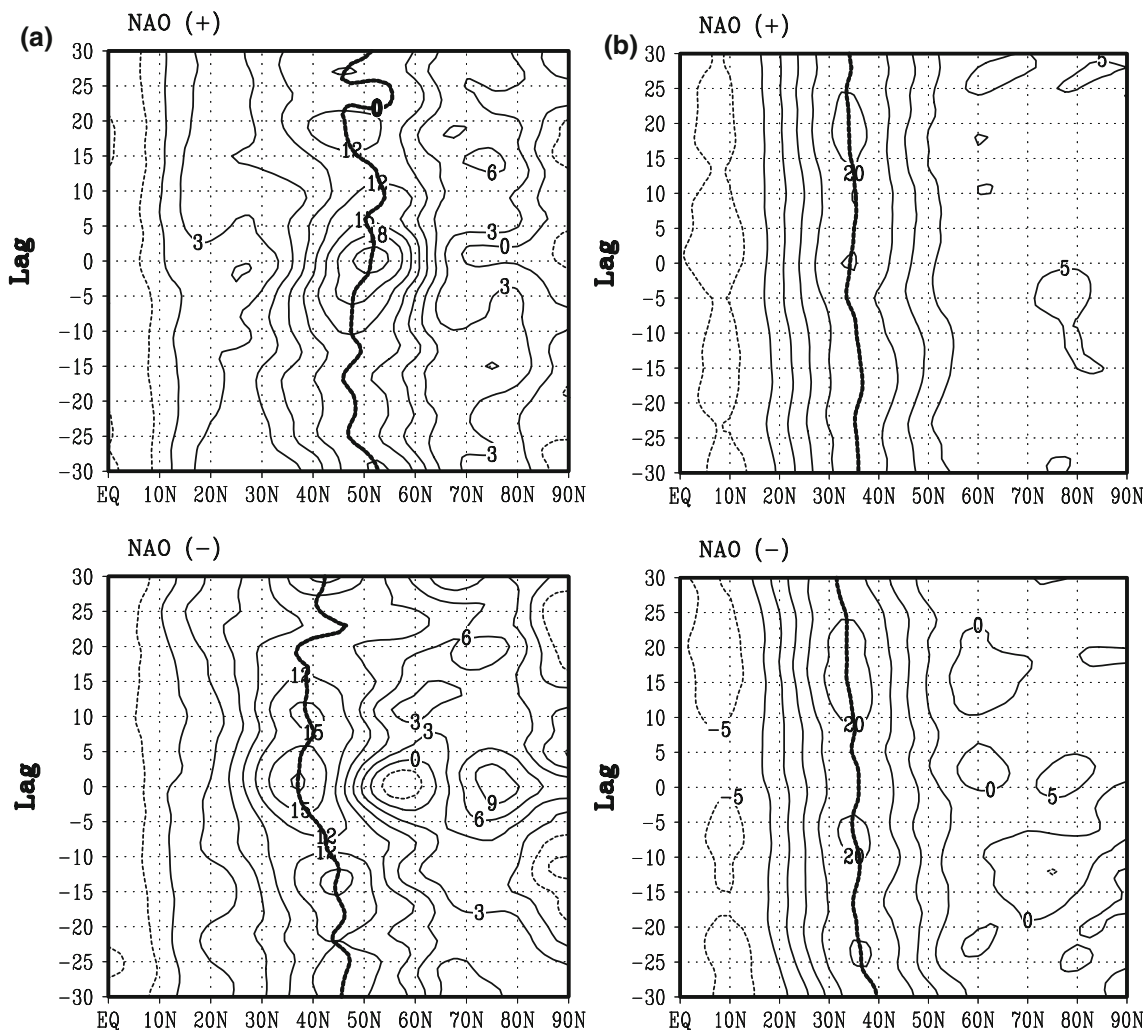
Fig. 1 Time and latitude evolution of vertical mean (from 1,000 to 300 hPa) zonal mean zonal winds during the life cycle of a composite NAO for its two phases, in which the thick solid line represents the jet core: **a** Atlantic basin and **b** Pacific basin

investigating the life cycle of eddy-driven NAO events in a localized shifting jet. Thus, it is necessary to further extend the weakly nonlinear NAO model proposed in Luo et al. (2008b) to include a localized shifting jet.

3 Linearized equivalent barotropic model and genesis of initial isolated dipole modes

3.1 Linearized equivalent barotropic model in a slowly varying jet flow

Since the NAO exhibits usually a barotropic vertical structure in the troposphere in the NH (Limpasuvan and Hartmann 1999; Thompson and Wallace 1998; Wallace 2000; Vallis et al. 2004), we can use an equivalent barotropic model to investigate the problems noted above.

The equivalent barotropic potential vorticity (PV) equation with both the localized vorticity forcing and the topography in a β-plane channel with a width of L_y can be written as (Pedlosky 1987)

$$\frac{\partial}{\partial t}(\nabla^2\psi - F\psi) + J(\psi, \nabla^2\psi + h_B) + \beta\frac{\partial\psi}{\partial x} = \nabla^2\psi_V^*, \quad (1)$$

where ψ is the non-dimensional streamfunction, $F = \left(\frac{L}{R_d}\right)^2$ and $\beta = \beta_0\frac{L^2}{U_0}$, in which β_0 is the latitudinal gradient of the Coriolis parameter at a reference latitude ϕ_0, R_d is the radius of Rossby deformation and assumed to equal to L (Luo et al. 2007a), $U_0 = 10$ m/s and $L = 1,000$ km are the characteristic scales of the horizontal velocity and length, respectively, $f_0 = 10^{-4}$ s^{-1} is a constant Coriolis parameter, h_B is the non-dimensional topographic variable scaled with 1,000 m, and $\nabla^2\psi_V^*$ is a localized vorticity forcing that is not affected by a perturbation.

In this section, we assume that this localized vorticity forcing is steady and drives the steady flow noted by $\bar{\psi}$ to satisfy the following constrain (Mak 2002):

$$J(\bar{\psi}, \nabla^2\bar{\psi}) + \beta\frac{\partial\bar{\psi}}{\partial x} = \nabla^2\psi_V^*. \tag{2}$$

In order to reflect the zonal variation of a westerly jet prior to the NAO in the NH, we assume that the zonally varying jet flow maintained by the external voricity forcing is of the form of $\bar{\psi} = \bar{\psi}(X, y)$ (where $X = \varepsilon x$ and ε is a small parameter). Although the boundary condition (BC) of the basic state differs from the no normal flow or wall BC usually employed in quasi-geostrophic (QG) β-plane models (Whitaker and Dole 1995), the BC proposed by Mak (2002) can be used as a constraint of the basic state flow. For this case, the jet flow BCs are assumed to be (Mak 2002):

$$\bar{\psi}(X, y)\big|_{X\to-\infty} = \bar{\psi}(X, y)\big|_{X\to\infty}, \ \bar{\psi}(X, y)\big|_{y=0}$$
$$= 0, \ \bar{\psi}(X, y)\big|_{y=L_y} = \bar{\psi}_C, \tag{3}$$

where $\bar{\psi}_C$ is an additional free parameter related to the presence of rigid lateral boundaries (Mak 2002), which is easily determined if a zonally varying jet is given as done in the next subsection.

Using Eqs.1 and 2 the linearized equivalent barotropic PV equation that describes a stationary wave anomaly forced by the topography can be obtained as

$$J(\bar{\psi}, q_A) + J(\psi_A, \bar{q}) + J(\bar{\psi}, h_B) = 0, \tag{4}$$

where $U(X, y) = -\frac{\partial\bar{\psi}}{\partial y}$ and $V(X, y) = \varepsilon\frac{\partial\bar{\psi}}{\partial X}$ are the zonal and meridional components of a localized shifting jet respectively, $q_A = \nabla^2\psi_A$, $\bar{q} = \frac{f_0 L}{U_0} + \beta y + \nabla^2\bar{\psi}$, and ψ_A is a stationary wave anomaly subject to the boundary conditions: $\psi_A\big|_{y=0} = \psi_A\big|_{y=L_y} = 0$ and $\psi_A(X, x, y)\big|_{X\to-\infty} = \psi_A(X, x, y)\big|_{X\to\infty}$.

In past many years the barotropic or baroclinic instability of a zonally varying flow has been widely investigated in various models (Pierrehumbert 1984; Mak 2002). When the basic flow is unstable, the disturbance would evolve toward a most unstable normal mode at large time (Mak 2002). However, a linearized stationary wave equation can be used as an initial-value model that provides an initial NAO structure even though its time-dependent solution may be unstable. This is because our emphasis is focused on the initial condition of the NAO anomaly rather than on the evolution of a time-dependent solution. As we will note later, the time-dependent evolution solution of an initial value can probably be predicted by a nonlinear equation in a weakly nonlinear framework if the stationary wave anomaly solution obtained from Eq. 4 is considered as an initial value.

3.2 Analytical solution of stationary wave anomaly in a north–south shifting jet

In the NH the stationary wave is usually excited by the large-scale topography in mid-high latitudes. As in Luo et al. (2007b), because the mid-high latitude topography in the NH is a wavy form and dominated by zonal wavenumber 2, it can be assumed to be of the form

$$h_B = h_0 \exp[ik(x + x_T)]\sin(my/2) + cc, \tag{5}$$

where $m = \pm\frac{2\pi}{L_y}$, h_0 is the amplitude of the wavy topography with the zonal wavenumber $k = 2k_0$ and $k_0 = 1/[6.371\cos(\phi_0)]$, x_T is the position of the topographic trough relative to $x = 0$, and cc denotes the complex conjugate of its preceding term. Note that when $m = \frac{2\pi}{L_y}$ ($m = -\frac{2\pi}{L_y}$) is chosen, there should be $h_0 < 0$ ($h_0 > 0$) so that the region around $x = 0$ represents the Atlantic basin. In addition, the parameters $L_y = 5$, $\varepsilon = 0.24$ and $\phi_0 = 55°N$ are fixed in the whole paper.

Generally speaking, the Atlantic jet mainly exists in the upstream side of the Atlantic basin where the strongest latitudinal shift of the jet takes place. Thus, in this paper we assume $\bar{\psi} = -u_0 y + \alpha_J\sin(my)/m - 2\alpha_S(X)\sin(my/2)/m$ so that $U = -\frac{\partial\bar{\psi}}{\partial y}$ is

$$U = u_0 - \alpha_J\cos(my) + \alpha_S(X)\cos(my/2), \tag{6}$$

where u_0 is a constant westerly wind, α_J represents the strength (pulsing) of the zonal jet, and $\alpha_S(X)$ denotes a localized meridional shift of the zonal jet. Also, it is easy to obtain $\bar{\psi}_C = -u_0 L_y$ in Eq. 3 using Eq. 6. In this paper, we assume that the westerly jet is not enough strong so that the barotropic instability of westerly jet is negligible even if the local instability is possible for a zonally varying jet flow with weak zonal variation (Swanson 2001). This allows us to analytically solve Eq. 4 as an initial value of the NAO anomaly.

Without the loss of generality, we assume $\alpha_S(X) = \alpha_{S0}\exp[-\sigma_0(X + \varepsilon x_\alpha)^2]$, where α_{S0} denotes the maximum shift of the zonal jet, σ_0 denotes the local extent of the jet, and x_α represents the position of the maximum of the jet relative to $x = 0$. For $\sigma_0 = 0$ this jet becomes uniform along the NH and is identical to that used by Luo et al. (2008b).

For the parameters $u_0 = 0.8$, $\sigma_0 = 0.48$, $x_\alpha = 0$ and $\alpha_J = 0.24$, the horizontal distribution of $U(X, y)$ is shown in Fig. 2 for $\alpha_{S0} = 0.24$, $\alpha_{S0} = 0$ and $\alpha_{S0} = -0.24$.

It is found that the jet is zonally localized for $\sigma_0 > 0$. But when $\alpha_{S0} < 0$ ($\alpha_{S0} > 0$), the zonal jet undergoes a localized northward (southward) shift (Fig. 2a, c). If $|\alpha_{S0}|$ is larger, the latitudinal shift of the zonal jet is more distinct (not shown). Thus, the different westerly jets can be obtained by modifying the parameter α_{S0}. It is true that this parameter modifies the latitude of the local jet but it

Fig. 2 Horizontal distributions of westerly jets for different types: **a** $\alpha_{S0} = -0.24$, **b** $\alpha_{S0} = 0$ and **c** $\alpha_{S0} = 0.24$
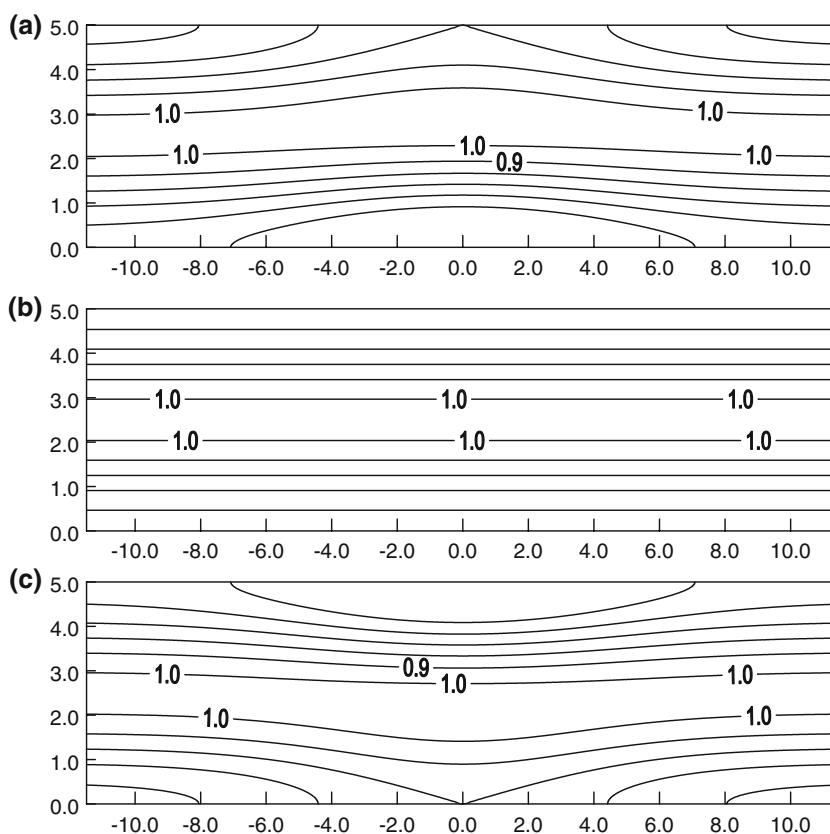
modifies also locally the difference between the cyclonic shear and the anticyclonic shear of the jet. In Fig. 2a, for the more northward jet, the anticyclonic shear is much stronger than the cyclonic shear. The reverse happens for the more southward jet in Fig. 2c. According to Thorncroft et al. (1993), this difference could explain why the more northward jet will favor anticyclonic wave breaking and the positive phase of the NAO and the more southward jet cyclonic wave breaking and the negative phase (Luo et al. 2008b). In particular, the zonal localization of the jet shift is enhanced as σ_0 is increased (not shown). Observation shows that in the NH a strongest latitudinal shift of the zonal jet prior to the NAO mainly takes place over the Atlantic basin (Fig. 1), thus suggesting that the zonal jet before a NAO life cycle begins should be zonally localized. Although the physical cause of the regional variability of the zonal jet is not clearly identified so far, some investigations suggested that the variability of the sea-surface temperature (SST) anomaly over the Gulf Stream region be one of the causes of the jet shift (Feliks et al. 2004). This problem is beyond the scope of this paper and deserves further exploration.

Let us suppose $\alpha_J = \varepsilon\tilde{\alpha}_J$ and $\alpha_{S0} = \varepsilon\tilde{\alpha}_{S0}$ so as to obtain analytical solution to Eq. 4. Through substituting $\bar{\psi}$ and Eq. 5 into Eq. 4, the asymptotic solution to Eq. 4 can be obtained as

$$\psi_A = \psi_{A0} + \psi_{A1}, \tag{7a}$$

$$\psi_{A0} = h_0 h_A \exp[ik(x + x_T)] \sin\left(\frac{m}{2}y\right) + cc, \tag{7b}$$

$$\psi_{A1} = \psi_{AT} + \psi_{AD} + \psi_{AM}, \tag{7c}$$

$$\psi_{AT} = \alpha_J \frac{[(-k^2 + \frac{3m^2}{4})h_A + 1]}{2u_0[\frac{\beta}{u_0} - (k^2 + \frac{9m^2}{4})]} h_0$$
$$\times \exp[ik(x + x_T)] \sin(3my/2) + cc, \tag{7d}$$

$$\psi_{AD} = -\frac{(-k^2 h_A + 1)}{2u_0[\frac{\beta}{u_0} - (k^2 + m^2)]} h_0 \alpha_S(\varepsilon x)$$
$$\times \exp[ik(x + x_T)] \sin(my) + cc, \tag{7e}$$

$$\psi_{AM} = -\alpha_J \frac{[(-k^2 + \frac{3m^2}{4})h_A + 1]}{2u_0[\frac{\beta}{u_0} - (k^2 + \frac{m^2}{4})]} h_0$$
$$\times \exp[ik(x + x_T)] \sin(my/2) + cc, \tag{7f}$$

where $\alpha_S(X) = \alpha_S(\varepsilon x)$ and $h_A = -\frac{1}{[\beta/u_0 - (k^2 + m^2/4)]}$, ψ_{AT}, ψ_{AD} and ψ_{AM} correspond in turn to tripole, dipole and monopole modes. Note that if $\alpha_S(\varepsilon x)$ is a constant Eq. 7 is identical to that derived by Luo et al. (2008b). It must be pointed out that there are three resonant points in Eq. 7: $u_{DC} = \frac{\beta}{k^2 + m^2}$, $u_{TC} = \frac{\beta}{k^2 + 9m^2/4}$ and $u_{MC} = \frac{\beta}{k^2 + m^2/4}$, where u_{DC}, u_{TC} and u_{MC} are the resonant westerly winds, respectively. It is

evident that there is $u_{TC} < u_{DC} < u_{MC}$. At 55°N we can have $u_{DC} \approx 0.7$ (7 m/s in a dimensional form), $u_{TC} \approx 0.341$ (3.41 m/s) and $u_{MC} \approx 1.98$ (19.8 m/s). The conditions $u_0 \neq u_{DC}$, $u_0 \neq u_{TC}$ and $u_0 \neq u_{MC}$ must be satisfied to insure that solution (Eq. 7) holds.

It is found that an interaction between the shifting jet and topographic wave ridge tends to result in three modes: tripole (ψ_{AT}), dipole (ψ_{AD}) and monopole (ψ_{AM}) modes. The amplitudes of these modes depend upon the setting of the uniform westerly wind u_0. When the jet shift is zonally localized, the dipole mode is zonally localized. In a weak background westerly wind u_0, the dipole mode is dominant compared to other two modes. There is generally $u_{TC} < u_0 < u_{MC}$ in mid-high latitudes (Fig. 1). Moreover, it is also seen that the condition $u_0 > u_{DC}$ can almost hold over the Atlantic basin for two phases of the NAO (not shown). In this case, the phase of the resulting dipole mode (ψ_{AD}) is dominated by the latitudinal shift of the prior Atlantic jet.

3.3 A link between the localized jet shift and genesis of initial isolated dipole modes

Here, we take the parameters $u_0 = 0.8$, $x_T = 0$, $x_\alpha = 0$, $\alpha_J = 0.24$ and $h_0 = -0.5$, but allow the varying of σ_0. For $\alpha_{S0} = 0.24$ and $\alpha_{S0} = -0.24$. Figure 3 shows the stationary wave anomalies ψ_A and ψ_{AD} for $\sigma_0 = 0$, but the cases of $\sigma_0 = 0.24$ and $\sigma_0 = 0.48$ are shown in Figs. 4 and 5, respectively.

It is found that when the zonal jet is more zonally localized, the dipole mode denoted by ψ_{AD} is more zonally isolated (Figs. 4, 5). Such dipole mode can have a low-over-high or high-over-low structure if the zonal jet undergoes a northward ($\alpha_{S0} = -0.24$) or southward ($\alpha_{S0} = 0.24$) shift. Also, the strength of the isolated dipole mode is proportional to the shift strength (α_{S0}) of a localized jet. If this dipole mode is regarded as the initial value of the NAO anomaly, the positive (negative) phase of the subsequent NAO pattern is inevitably determined by the

Fig. 3 Horizontal distributions of stationary wave anomalies ψ_A and ψ_{AD} for a uniform latitudinally shifting jet ($\sigma_0 = 0$) [Contour interval (CI) is 0.2], in which **a** and **b** or **c** and **d** corresponds to a southward ($\alpha_{S0} = 0.24$) or northward ($\alpha_{S0} = -0.24$) shifting jet: **a** ψ_A field; **b** ψ_{AD} field; **c** ψ_A field and **d** ψ_{AD} field
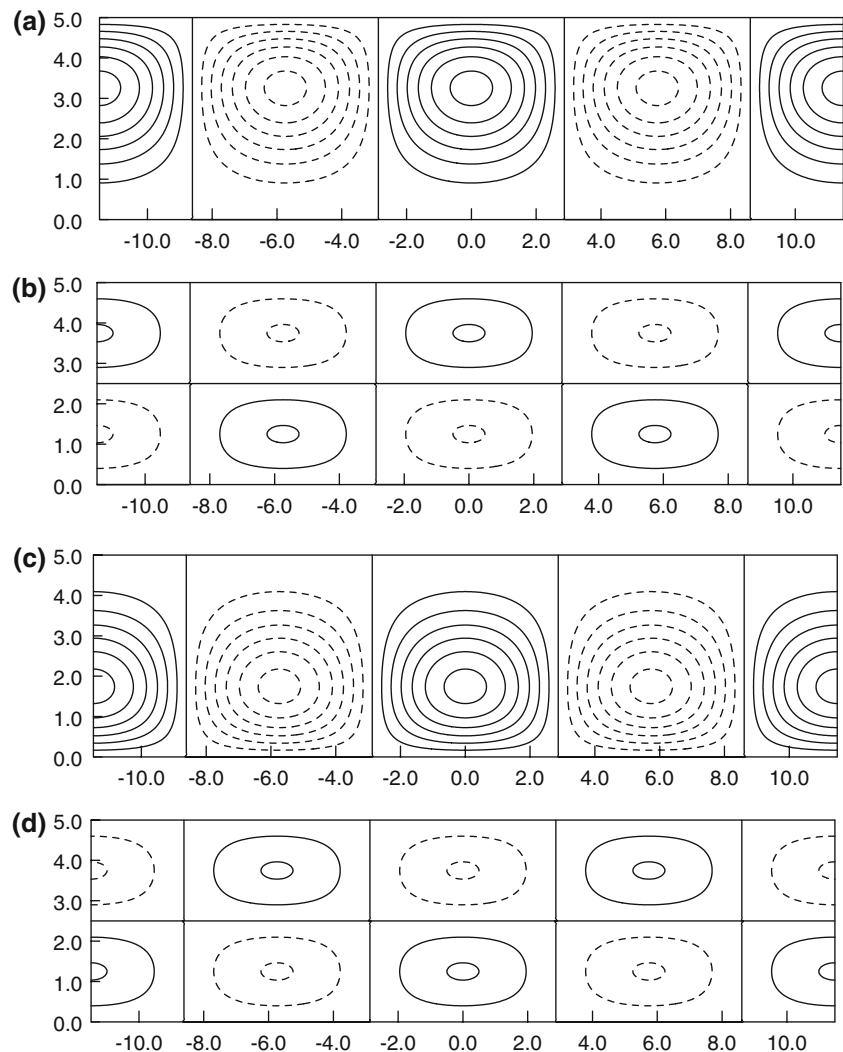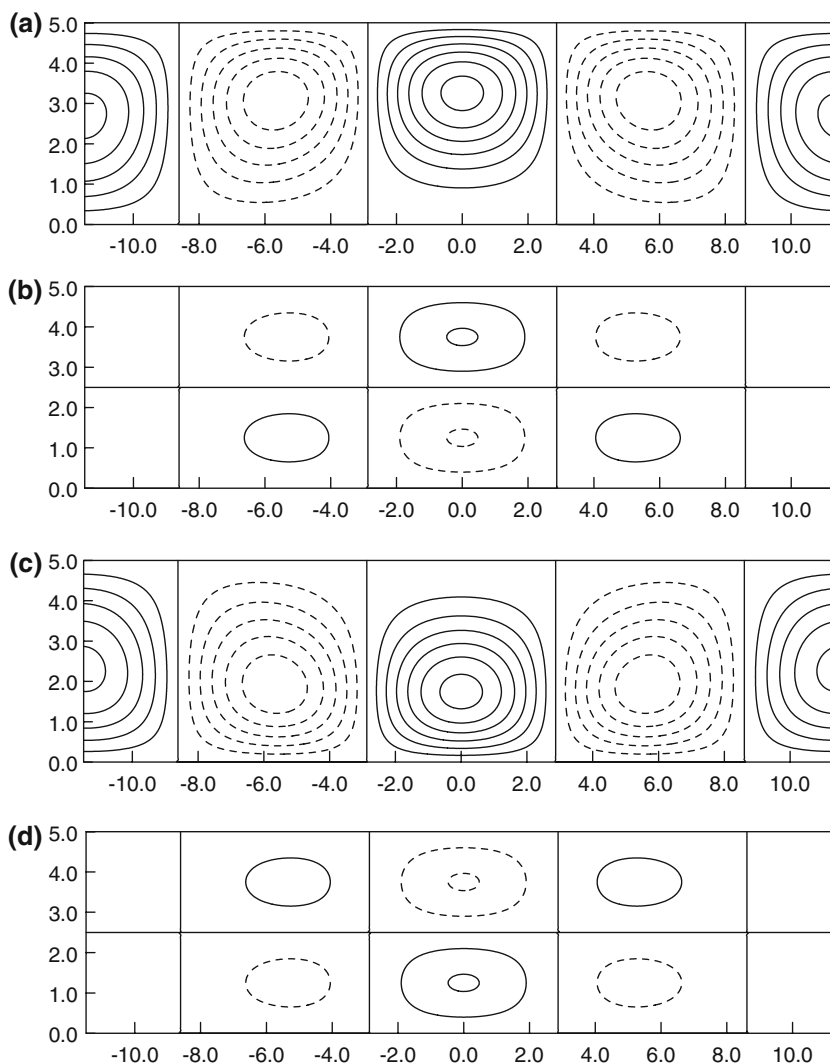
Fig. 4 As Fig. 3 for $\sigma_0 = 0.24$

northward (southward) shift of the prior Atlantic jet. It is also obvious that when the uniform westerly wind u_0 is increased for $u_0 > u_{DC}$, the amplitude of the dipole mode is reduced, but concurrently the amplitudes of both the tripole and monopole modes are enhanced (not shown). In subsequent sections, the excited dipole modes are considered as the initial values of the NAO anomaly in a weakly nonlinear model.

4 Weakly nonlinear model of NAO events in a localized shifting jet

It has been demonstrated previously that the dipole mode can arise from the interaction between the shifting jet and topographic stationary wave, which provides an initial value of the NAO anomaly (Luo et al. 2008b). In this

section, we will directly extend the weakly nonlinear NAO model in Luo et al. (2008b) to include a localized shifting jet in order to clarify how the initial conditions and the eddy distribution affect the zonal structure of eddy-driven NAO anomalies in a localized shifting jet.

4.1 Planetary wave-eddy interaction model in a localized shifting jet

In this section, the zonally varying jet flow denoted by $\bar{\psi}(X, y)$ is assumed to be a background of the NAO life cycle. In other words, this jet flow is considered as a localized jet prior to the NAO. As done in Luo et al. (2007a, b, 2008a, b), in a zonally varying jet flow $\bar{\psi}(X, y)$ the non-dimensional planetary (ψ) and synoptic (ψ') wave equations can be obtained as

Fig. 5 As Fig. 3 but for $\sigma_0 = 0.48$
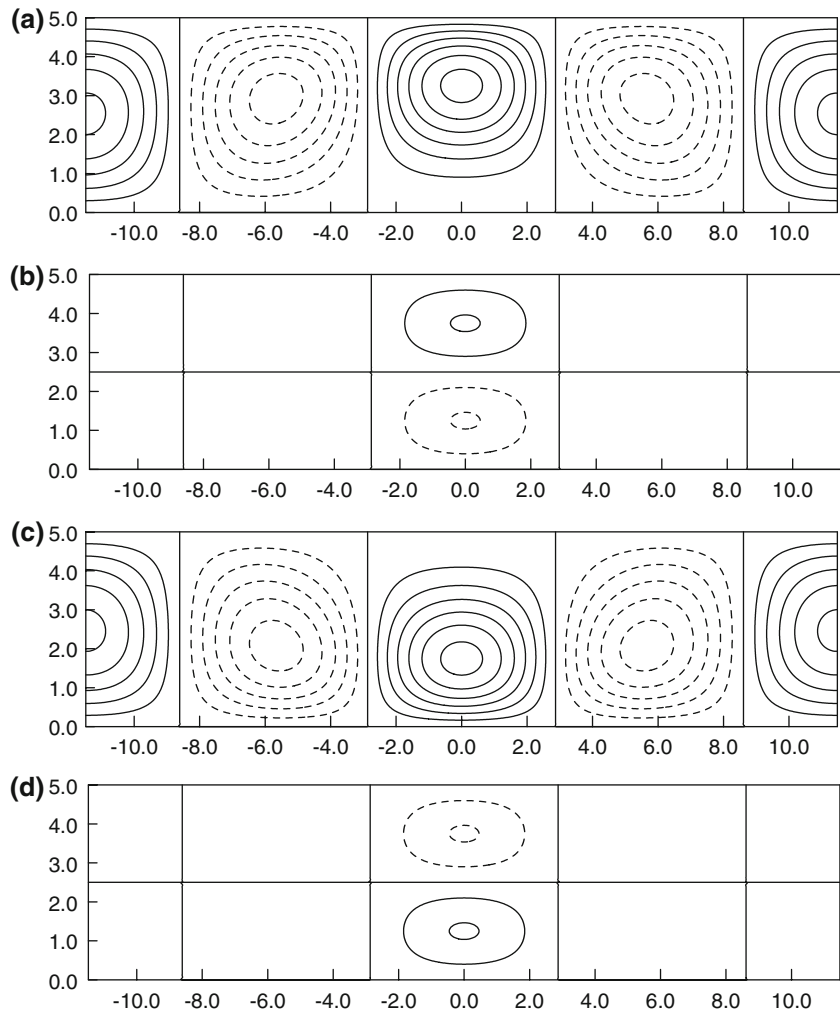
$$\left(\frac{\partial}{\partial t} + U\frac{\partial}{\partial x}\right)(\nabla^2\psi - F\psi) + J(\psi, \nabla^2\psi + h_B)$$
$$+ \left(\beta + FU + \frac{\partial}{\partial y}\nabla^2\bar{\psi}\right)\frac{\partial\psi}{\partial x} + U\frac{\partial h_B}{\partial x}$$
$$= -\varepsilon\frac{\partial\bar{\psi}}{\partial X}\frac{\partial}{\partial y}(\nabla^2\psi + h_B) + \frac{\partial\psi}{\partial y}\varepsilon\frac{\partial}{\partial X}\nabla^2\bar{\psi} - J(\psi', \nabla^2\psi')_P,$$

(8a)

$$\left(\frac{\partial}{\partial t} + U\frac{\partial}{\partial x}\right)(\nabla^2\psi' - F\psi') + \left(\beta + FU + \frac{\partial}{\partial y}\nabla^2\bar{\psi}\right)\frac{\partial\psi'}{\partial x}$$
$$= -\varepsilon\frac{\partial\bar{\psi}}{\partial X}\frac{\partial}{\partial y}\nabla^2\psi' + \frac{\partial\psi'}{\partial y}\varepsilon\frac{\partial}{\partial X}\nabla^2\bar{\psi}$$
$$- J(\psi', \nabla^2\psi + h_B) - J(\psi, \nabla^2\psi') + \nabla^2\psi_S^*,$$

(8b)

where $\nabla^2\bar{\psi} = \varepsilon^2\frac{\partial^2\bar{\psi}}{\partial X^2} + \frac{\partial^2\bar{\psi}}{\partial y^2}$, $J(\psi', \nabla^2\psi')_P$ is the planetary-scale component of the synoptic eddy vorticity fluxes, and denotes an eddy vorticity forcing in the Atlantic storm track which reflects the strength and longitudinal distribution of preexisting synoptic-scale eddies, $\nabla^2\psi_S^*$ is the

synoptic-scale vorticity source introduced to maintain the preexisting synoptic-scale eddies and other notation can be found in Luo et al. (2008b). If one assumes $\bar{\psi}(X, y) = -u_0 y$, Eq. 8 is reduced to that obtained by Luo et al. (2007a, b, 2008a, b) based upon a scale separation assumption.

4.2 Nonlinear planetary- and synoptic-scale solutions of a NAO life cycle and the associated nonlinear NAO evolution equation

In this section we have three reasons to make an assumption that there are both $\alpha_J = \varepsilon\tilde{\alpha}_J$ and $\alpha_S(X) = \varepsilon^2\tilde{\alpha}_S(X)$, based upon the observational fact as shown in Fig. 1. Although the NAO describes the meridional shift of a jet during its life cycle, the variability of the zonal jet prior to the NAO is relatively robust in strength compared to in position (Fig. 1). This assumption is roughly valid for the life cycle of a NAO event because $U(X, y)$ has been
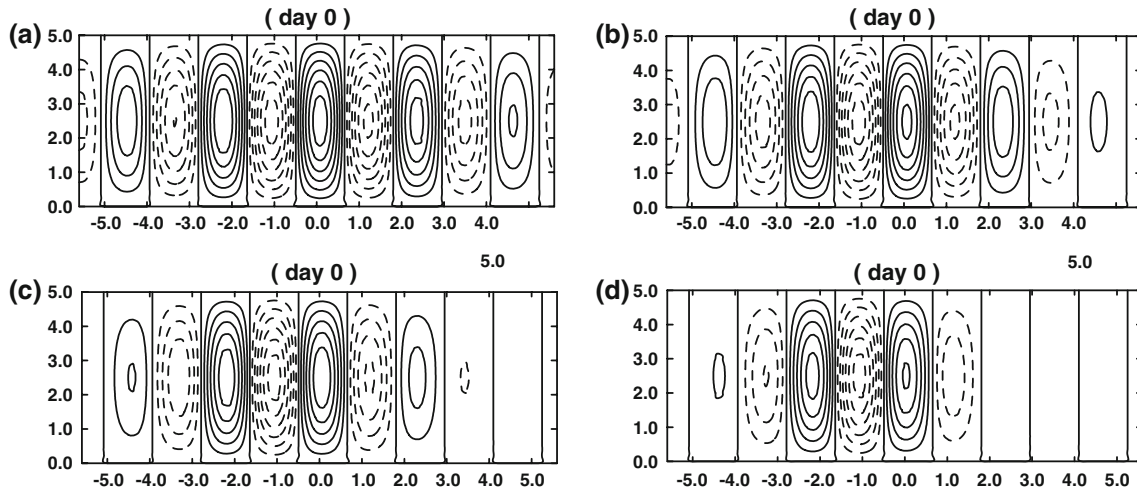
Fig. 6 Horizontal distribution of preexisting synoptic-scale eddies ψ'_0 at day 0 (CI = 0.1): **a** $\mu = 0.12$, **b** $\mu = 0.6$, **c** $\mu = 1.2$ and **d** $\mu = 2.4$

assumed to be a localized jet before a NAO life cycle begins. In our subsequent asymptotic solutions the jet variation associated with the NAO can be expressed by other variables, rather than by $U(X, y)$. Secondly, this assumption can avoid the resonant point at $u_0 = u_{DC}$ of the topographic dipole mode. It can also make term $\alpha_S(X)$ disappear in lowest order linear equation while it can appear in the higher order equations. Such an assumption can avoid the linear instability of barotropic flow at the lowest order due to the weak zonal variation of the pre-scribed jet (Pierrehumbert 1984).

According to Luo et al. (2007a, b), under $u_0 = u_{DC}$ the planetary-scale solution of a NAO life cycle in a localized shifting jet can be obtained in a fast-variable form as

$$\psi_P = \bar{\psi} + \psi \approx -u_0 y + \alpha_J \frac{\sin(my)}{m} - \alpha_S(\varepsilon x) \frac{2 \sin(my/2)}{m}$$
$$+ \psi_W + \psi_m, \tag{9a}$$

$$\psi_W = \psi_{NAOA} + \psi_{NAOB} + \psi_{C1} + \psi_{C2}, \tag{9b}$$

$$\psi_{NAOA} = B \sqrt{\frac{2}{L_y}} \exp(ikx) \sin(my) + cc, \tag{9c}$$

$$\psi_{NAOB} = -\alpha_J \frac{k^2}{2u_0 \left[\frac{\beta}{u_0} - (k^2 + 4m^2) \right]}$$
$$\times B \sqrt{\frac{2}{L_y}} \exp(ikx) \sin(2my) + cc, \tag{9d}$$

$$\psi_{C1} = h_A h_0 \exp[ik(x + x_T)] \sin(\frac{m}{2}y) + cc, \tag{9e}$$

$$\psi_{C2} = \psi_{AT} + \psi_{AM}, \tag{9f}$$

$$\psi_m = \psi_{m1} + \psi_{m2}, \tag{9g}$$

$$\psi_{m1} = -|B|^2 \sum_{n=1}^{\infty} q_n g_n \cos(n + 1/2)my, \tag{9h}$$

$$\psi_{m2} = -h_0 h_A \sqrt{\frac{2}{L_y}} (B e^{-ikx_T} + B^* e^{ikx_T})$$
$$\times \sum_{n=1}^{\infty} \tilde{q}_n (3a_n - b_n) \cos(nmy), \tag{9i}$$

where $B(x, t)$ is the amplitude of the eddy-driven NAO anomaly ψ_{NAOA}, ψ_{AT} and ψ_{AM} are the same as Eqs. 7d and 7f, and other coefficients can be found in Luo et al. (2007a, b, 2008a, b). Note in passing that the solutions presented in Eq. 9 are obtained under $u_0 = u_{DC}$. Because of the assumption $\alpha_S(X) = \varepsilon^2 \tilde{\alpha}_S(X)$, the solution ψ_{AD} in Eq. 7 does not appear in Eq. 9. Instead, this dipole mode due to the interaction between the localized shifting jet and a topographic stationary wave can appear in higher order equations. In this regard, the impact of the localized shifting jet on the time-evolution of the NAO pattern can, to some extent, be reflected by a generalized Schrödinger equation with a jet shift term.

At the same time, the synoptic-scale solution of a NAO life cycle can be obtained in a fast-variable form as

$$\psi' \approx \varepsilon^{3/2} (\tilde{\psi}'_0 + \varepsilon \tilde{\psi}'_1) = \psi'_0 + \psi'_1 + \psi'_{flow}, \tag{10a}$$

$$\psi'_0 = f_0(x) \{ \exp[i(\tilde{k}_1 x - \tilde{\omega}_1 t)] + \alpha \exp[i(\tilde{k}_2 x - \tilde{\omega}_2 t)] \}$$
$$\times \sin \left(\frac{m}{2} y \right) + cc, \tag{10b}$$

$$\psi_1' = -\frac{m}{4}\sqrt{\frac{2}{L_y}}Q_1 B f_0 \exp\{i[(\tilde{k}_1+k)x-\tilde{\omega}_1 t]\}$$

$$\times\left[p_1\sin\left(\frac{3m}{2}y\right)+r_1\sin\left(\frac{m}{2}y\right)\right]$$

$$-\alpha\frac{m}{4}\sqrt{\frac{2}{L_y}}Q_2 B f_0 \exp\{i[(\tilde{k}_2+k)x-\tilde{\omega}_2 t]\}$$

$$\times\left[p_2\sin\left(\frac{3m}{2}y\right)+r_2\sin\left(\frac{m}{2}y\right)\right]$$

$$+\frac{m}{4}\sqrt{\frac{2}{L_y}}Q_1 B^* f_0 \exp\{i[(\tilde{k}_1-k)x-\tilde{\omega}_1 t]\}$$

$$\times\left[s_1\sin\left(\frac{3m}{2}y\right)+h_1\sin\left(\frac{m}{2}y\right)\right]$$

$$+\alpha\frac{m}{4}\sqrt{\frac{2}{L_y}}Q_2 B^* f_0 \exp\{i[(\tilde{k}_2-k)x-\tilde{\omega}_2 t]\}$$

$$\times\left[s_2\sin\left(\frac{3m}{2}y\right)+h_2\sin\left(\frac{m}{2}y\right)\right]$$

$$-\frac{m}{4}f_0 h_0 \pi_1 \exp\{i[(\tilde{k}_1+k)x+kx_T-\tilde{\omega}_1 t]\}\sin(my)$$

$$-\alpha\frac{m}{4}f_0 h_0 \pi_2 \exp\{i[(\tilde{k}_2+k)x+kx_T-\tilde{\omega}_2 t]\}\sin(my)$$

$$-\frac{m}{4}f_0 h_0 \sigma_1 \exp\{i[(\tilde{k}_1-k)x-kx_T-\tilde{\omega}_1 t]\}\sin(my)$$

$$-\alpha\frac{m}{4}f_0 h_0 \sigma_2 \exp\{i[(\tilde{k}_2-k)x-kx_T-\tilde{\omega}_2 t]\}\sin(my)+cc,$$
$$(10c)$$

$$\psi_{flow}' = \frac{\alpha_J}{2}f_0(x)\{\Theta_1\exp[i(\tilde{k}_1 x-\tilde{\omega}_1 t)]$$

$$+\alpha\Theta_2\exp[i(\tilde{k}_2 x-\tilde{\omega}_2 t)]\}\sin(\frac{3m}{2}y)+cc,\qquad(10d)$$

where $\Theta_i = \dfrac{\tilde{k}_i\left(\frac{3m^2}{4}-\tilde{k}_i^2\right)}{(\beta+Fu_0)\tilde{k}_i-\left[\tilde{k}_i^2+\left(\frac{3m}{2}\right)^2+F\right](u_0\tilde{k}_i-\tilde{\omega}_i)}$,

$\tilde{\omega}_i = u_0\tilde{k}_i - \frac{(\beta+Fu_0)\tilde{k}_i}{\tilde{k}_i^2+m^2/4+F}$ $(i=1,2)$, $\alpha = \pm1, f_0(x) = a_0\exp[-\mu\varepsilon^2(x+x_0)]$ is the zonal distribution of preexisting synoptic-scale eddies, in which a_0 is the eddy strength, μ denotes the zonal localization of the synoptic eddy and the other notation and coefficients can be found in Luo et al. (2007a, b, 2008a, b).

It is noted that Eqs. 9 and 10 represent the planetary- and synoptic solutions of a negative phase NAO life cycle if $m = -\frac{2\pi}{L_y}$, $\alpha = -1$ and $h_0 = 0.5$ are chosen. But when $m = \frac{2\pi}{L_y}$, $\alpha = 1$ and $h_0 = -0.5$ are chosen, they denote the solutions of a positive phase. On the other hand, the impact of the localized latitudinal shift of the jet on the synoptic-scale eddies has been neglected because of $\alpha_S(X) = \varepsilon^2\tilde{\alpha}_S(X)$. The analytical solutions presented in Eqs. 9 and 10 are naturally an extension of the planetary- and synoptic-scale solutions of a NAO life cycle derived by Luo et al. (2008b).

If the equation of the NAO amplitude $B(x, t)$ can be obtained and solved, the planetary- and synoptic-scale evolutions of the NAO life cycle can be predicted in terms of Eqs. 9 and 10.

Following Luo et al. (2007a, b, 2008b), the NAO amplitude $B(x, t)$ can evolve according to

$$i\left(\frac{\partial B}{\partial t}+C_g\frac{\partial B}{\partial x}\right)+\lambda\frac{\partial^2 B}{\partial x^2}+\delta|B|^2 B+\tilde{\alpha}h_0^2(B+B^*e^{i2kx_T})$$

$$+\gamma_\rho\alpha_{\text{shift}}(\varepsilon x)h_0\exp(ikx_T)+H_\alpha\alpha_J^2 B$$

$$+Gf_0^2\exp[-i(\Delta kx+\Delta\omega t)]=0,\qquad(11)$$

where $H_\alpha = -\dfrac{k^3(k^2+3m^2)}{4u_0\left[\frac{\beta}{u_0}-(k^2+4m^2)\right](k^2+m^2+F)}$, and other coefficients can be found in Luo et al. (2007a, b, 2008b).

It is found that when $H_\alpha\alpha_J^2 B$ is neglected and when $\alpha_S(\varepsilon x)$ is a constant (Eq. 11) is identical to that derived by Luo et al. (2008b). This generalized equation is able to describe how an initial dipole mode develops into a NAO pattern under the forcing of synoptic-scale eddies if both the initial NAO condition and preexisting synoptic-scale eddies are given. It is also noted that the jet shift plays no role if the topography is absent. The spatial-temporal evolution of the NAO life cycle in both planetary- and synoptic-scale fields can be identified if the solution (Eq. 11) can be obtained for any initial values. In this paper, a finite-difference scheme used by Luo et al. (2007a) is used to solve Eq. 11.

4.3 Jet variability in a response to the NAO life cycle

If a NAO life cycle occurs, a change in the zonal jet is inevitable due to the feedback of the NAO anomaly. Using Eq. 9, in a fast-variable form the modified zonal mean westerly wind associated with the NAO anomaly can be obtained as

$$u_m = U(\varepsilon x, y) + u_{\text{NAO}} + u_{\text{Interaction}},\qquad(12a)$$

$$u_{\text{NAO}} = -|B|^2\sum_{n=1}^{\infty}q_n g_n(n+1/2)m\sin(n+1/2)my,\qquad(12b)$$

$$u_{\text{Interaction}} = -h_0 h_A\sqrt{\frac{2}{L_y}}(Be^{-ikx_T}+B^*e^{ikx_T})$$

$$\times\sum_{n=1}^{\infty}\tilde{q}_n(3a_n-b_n)(nm)\sin(nmy).\qquad(12c)$$

It is noted that the jet variability consists of three parts: $U(\varepsilon x, y)$, u_{NAO} and $u_{\text{Interaction}}$, in which $U(\varepsilon x, y)$ is a time-independent localized jet prior to the NAO, u_{NAO} denotes a double-jet anomaly induced by the feedback of the NAO anomaly itself, but $u_{\text{Interaction}}$ represents the westerly jet anomaly induced by the interaction between the NAO anomaly and a topographic wave ridge over the Atlantic

basin. Thus, $u_{\text{NAO}} + u_{\text{Interaction}}$ represents actually the jet variability in both position and strength during the NAO life cycle.

It is likely that Eq. 12 can identify how the jet variability responds to the evolution of a NAO pattern if $B(x, t)$ is solved. The regional variability of the zonal jet is dominated by the eddy-driven NAO anomaly ψ_{NAOA} because both u_{NAO} and $u_{\text{Interaction}}$ contain its amplitude $B(x, t)$.

5 Isolated structure and zonal asymmetry of eddy-driven NAO anomaly

In this paper, the positive phase NAO is considered as an example. Without the loss of generality we choose the parameters as shown in Table 1, but allow the varying of μ so that its different values can represent the different distributions of the preexisting synoptic-scale eddies in the zonal direction. Moreover, α_{S0} is allowed to vary so as to permit the different meridional shift of a localized jet.

Figure 6 shows the horizontal distribution of preexisting synoptic-scale eddies ψ'_0 for different μ. It is easy to find that each component $\tilde{k}_i$ ($i = 1, 2$) of preexisting synoptic-scale eddies is almost zonally uniform if $\mu = 0.12$ is chosen. However, the preexisting storm track is more zonally localized if μ is increased (Fig. 6c, d). This is because the region of the maximum eddy kinetic energy of the synoptic-scale eddies is usually defined as the storm track. Thus, the zonal distribution of synoptic-scale eddies as shown in Fig. 6 can represent the longitudinal distribution of the Atlantic storm track. In the North Atlantic sector, the storm track organized by the preexisting synoptic-scale eddies is generally zonally localized due to the presence of the Rocky mountains, temperature contrast between the cold continent and warm ocean (Vallis and Gerber 2008), which is usually located at the upstream side of the Atlantic basin. Although, this storm track may differ for different winters because the thermal contrast is

different, Fig. 6c and d can basically reflect the commonly observed storm track in the Atlantic basin.

In this section, to see how the zonal structure of the eddy-driven NAO anomaly depends upon the initial conditions, without the loss of generality we choose $B(x, 0) = 0.4e^{-\gamma x^2}$ for $\gamma \geq 0$ as the initial value of the NAO anomaly, where $\gamma = 0$ denotes a uniform initial condition. Although $B(x, 0) = 0.4e^{-\gamma x^2}$ is highly idealized, $\gamma = 0$ and $\gamma = 0.08$ correspond approximately to the dipole mode structures shown in Figs. 3 and 5, respectively. In this paper, we only consider a positive phase NAO (NAO$^+$) anomaly as an example.
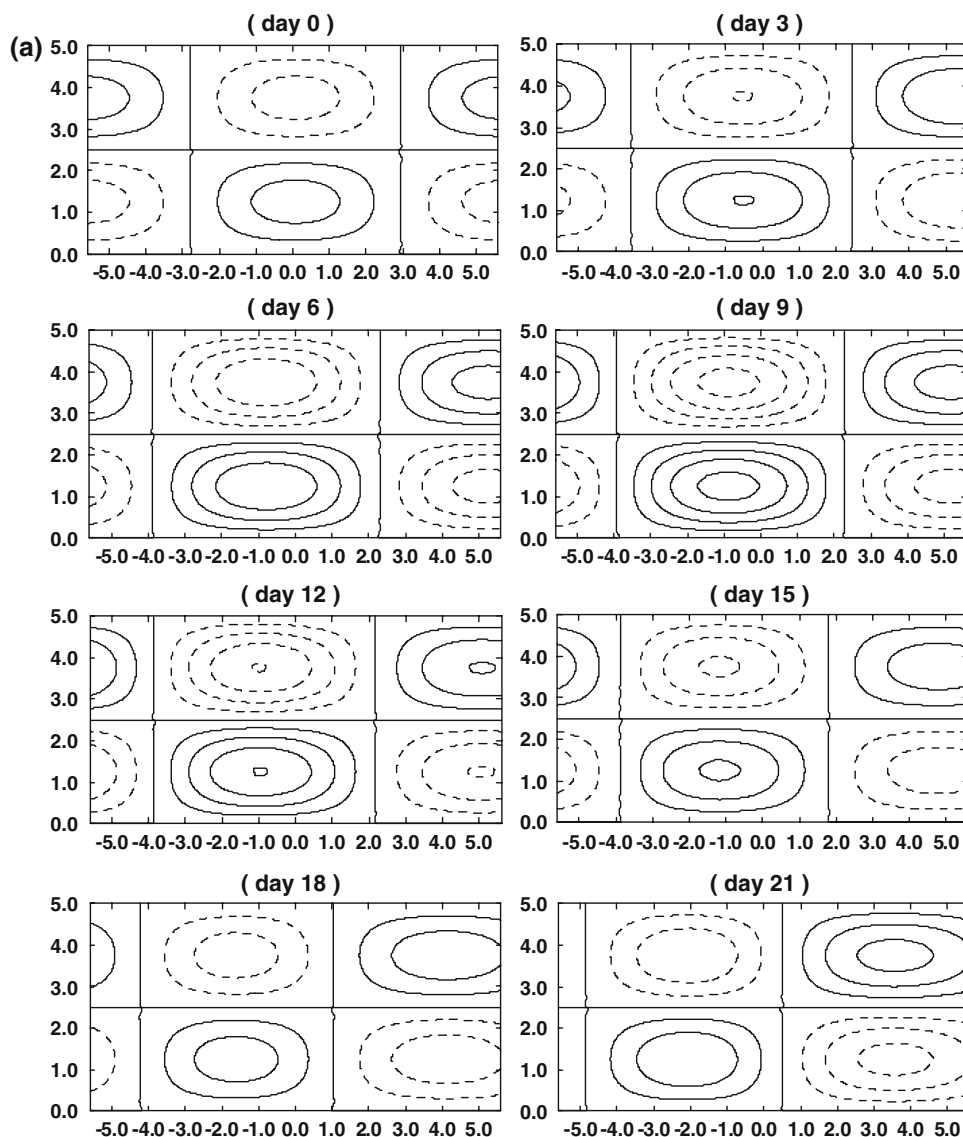
5.1 Isolated structure of eddy-driven NAO anomaly

For $B(x, 0) = 0.4$, we show the anomaly field ψ_{NAOA} of the NAO$^+$ life cycle without the effect of topographic wave anomaly ($h_0 = 0$) in a symmetric jet ($\alpha_{S0} = 0$) in Fig. 7 under the forcing of preexisting synoptic eddies for $\mu = 0.12$, $\mu = 2.4$ and $\mu = 4.8$. It is easily found that when the Atlantic storm track, organized by the preexisting synoptic-scale eddies, is almost zonally uniform, the resulting NAO$^+$ anomaly is not distinctly isolated in that the amplitude of the NAO$^+$ anomaly is still rather robust outside the Atlantic basin (Fig. 7a). However, the resulting NAO$^+$ anomaly can be zonally isolated, but depends upon the zonal localization of the preexisting eddies. This isolated pattern of the NAO$^+$ anomaly is enhanced when the preexisting synoptic-scale eddies are more zonally localized (Fig. 7b, c), in agreement with the numerical result of Vallis et al. (2004), who found that if the stirring forcing is enhanced in a zonally localized region, the resulting variability pattern is zonally localized, resembling a NAO$^+$ pattern. It is, however, obvious that the NAO anomaly is not sufficiently isolated in the zonal direction even though the preexisting eddies are sufficiently localized. This result is not found in a stochastic forcing model of the NAO and annular modes proposed by Vallis et al. (2004). Figure 8

Table 1 List of prescribed parameters in a weakly nonlinear solution

Parameters	Values
Jet strength α_J	0.24
Jet shift strength α_{S0}	0, 0.15, −0.15
Zonal extent of the localized jet σ_0	0.096
Position of the maximum jet shift x_a	0
Topographic height h_0	−0.5
Position of positive topographic wave anomaly x_T	−2.0
Wavenumbers of synoptic eddies $\tilde{k}_i$ ($i = 1, 2$)	As in Luo et al. (2007a)
Eddy strength a_0	0.17
Position of the maximum eddy strength x_0	2.87/2
Zonal distribution of synoptic-scale eddies μ	0.12, 2.4, 4.8

Fig. 7 Anomaly field ψ_{NAOA} of the positive-phase NAO life cycle in a symmetric jet ($\alpha_{S0} = 0$) for an initial value of $B(x, 0) = 0.4$ under the forcing of preexisting localized synoptic-scale eddies with different zonal distributions (CI = 0.2): **a** $\mu = 0.12$, **b** $\mu = 2.4$ and **c** $\mu = 4.8$


shows the case of the initial amplitude $B(x, 0) = 0.4e^{-0.08x^2}$ for the same parameters as in Fig. 7. A comparison with Fig. 7 shows that the spatial structure of the eddy-driven NAO anomaly is dominated by the initial value of the NAO anomaly itself. If the initial NAO anomaly is zonally isolated, the resulting NAO anomaly will be more zonally isolated. In other words, the isolated pattern of the eddy-driven NAO anomaly is enhanced if the initial NAO anomaly is concentrated in a zonally localized region. Thus, the spatial structure of the eddy-driven NAO anomaly is also dominated by the initial value of the NAO anomaly, indicating that the NAO life cycle is a nonlinear initial value problem (Benedict et al. 2004; Franzke et al. 2004). On the other hand, we can also see that the strength of the resulting NAO anomaly is relatively weak when the initial NAO anomaly is more zonally isolated. Thus, the occurrence of the isolated NAO anomaly is a natural

consequence of the interaction between the localized dipole mode over the Atlantic basin and localized Atlantic storm track.

5.2 Zonal asymmetry of eddy-driven NAO anomaly

It is easy to see that when the initial NAO anomaly is almost zonally uniform, the eddy-driven NAO anomaly is almost zonally symmetric along the longitude (Fig. 7a). The zonal asymmetry of the NAO anomaly appears to be more enhanced as the preexisting synoptic eddies are more zonally localized (Fig. 7b, c). This is consistent with the result of Cash et al. (2005), who found a roughly linear relationship between the zonal asymmetry of the EOF annular mode and the zonal localization of the storm track. However, in our theoretical model the zonal asymmetry of the NAO anomaly is also found to depend upon the initial

Fig. 7 continued
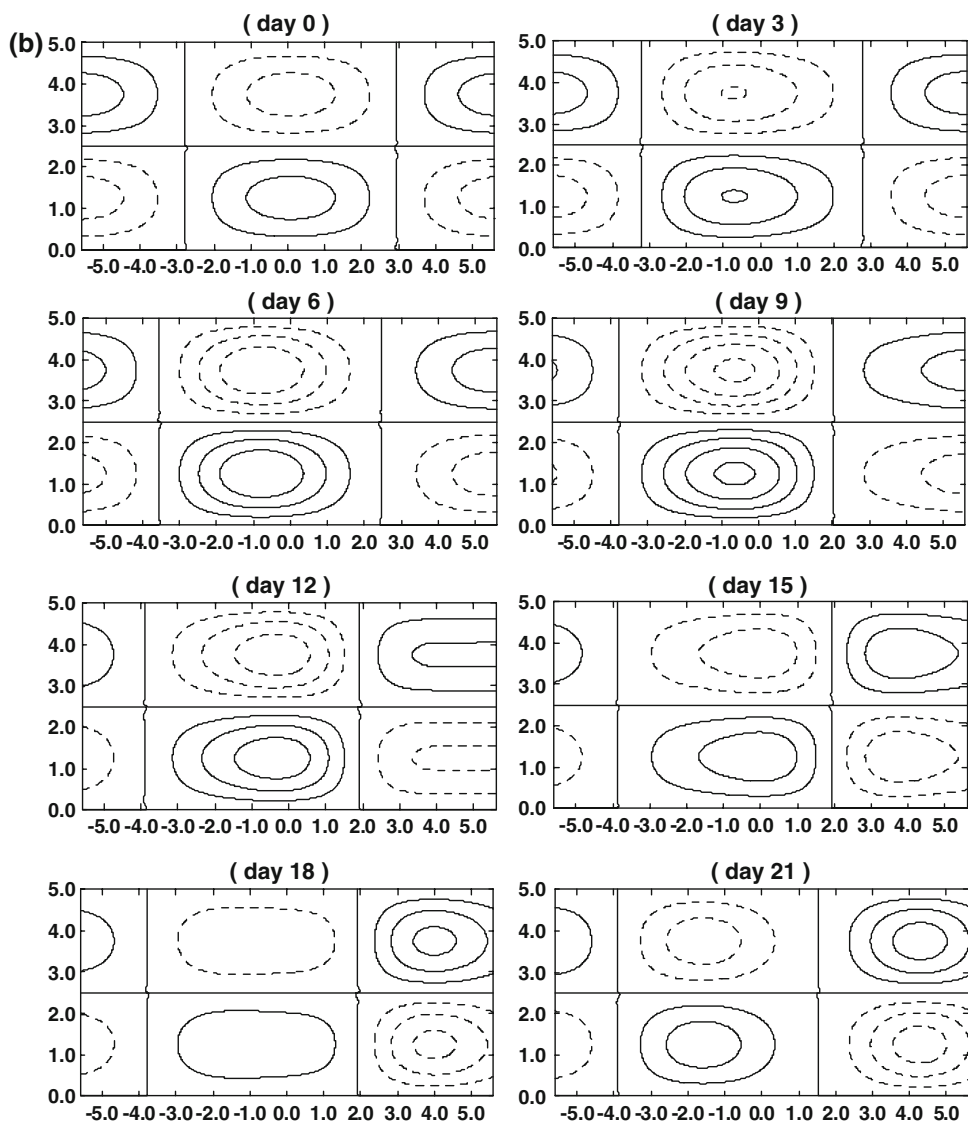
value itself. It is evident that there is a strong zonal asymmetry of the eddy-driven NAO anomaly as the initial NAO anomaly is zonally localized (Fig. 8a). This is because the large amplitude part of the isolated NAO anomaly propagates westward more rapidly than the small amplitude one so that the large amplitude part overtakes the small one (not shown). In this case, a zonal asymmetry of the resulting NAO anomaly will be inevitable. Generally speaking, because the prior Atlantic jet is zonally localized (Fig. 1), the initial NAO anomaly that arises from interaction between the prior jet and topographic stationary wave should be zonally localized (Figs. 4, 5). Thus, it is likely that the eddy- driven NAO anomaly can exhibit a strong zonal asymmetry.

For the same parameters as in Fig. 8, Fig. 9 shows the eddy-driven NAO anomaly with the effect of a topographic wave anomaly in a northward shifting jet ($\alpha_{S0} = -0.15$). It is noted that the zonal asymmetry of the NAO anomaly seems to be stronger in the presence of a topographic wave anomaly than in the absence of a topographic wave anomaly and is enhanced as the topographic height increases. This is because an increase in the height of topography can enhance the amplitude of the NAO anomaly, thus easily producing a strong zonal asymmetry of the NAO pattern. This zonal asymmetry is particularly evident during the decay phase when the preexisting synoptic-scale eddies are more zonally localized (Fig. 9b, c). Although Cash et al. (2005) noted that the presence of zonally asymmetric lower boundary conditions including a Gaussian topography can enhance the zonal asymmetry of the NAO anomaly, here we further find that the enhancement of the zonal asymmetry of the NAO anomaly in the presence of land-ocean continent topography does not only depend on the topographic height, but also on the initial

Fig. 7 continued
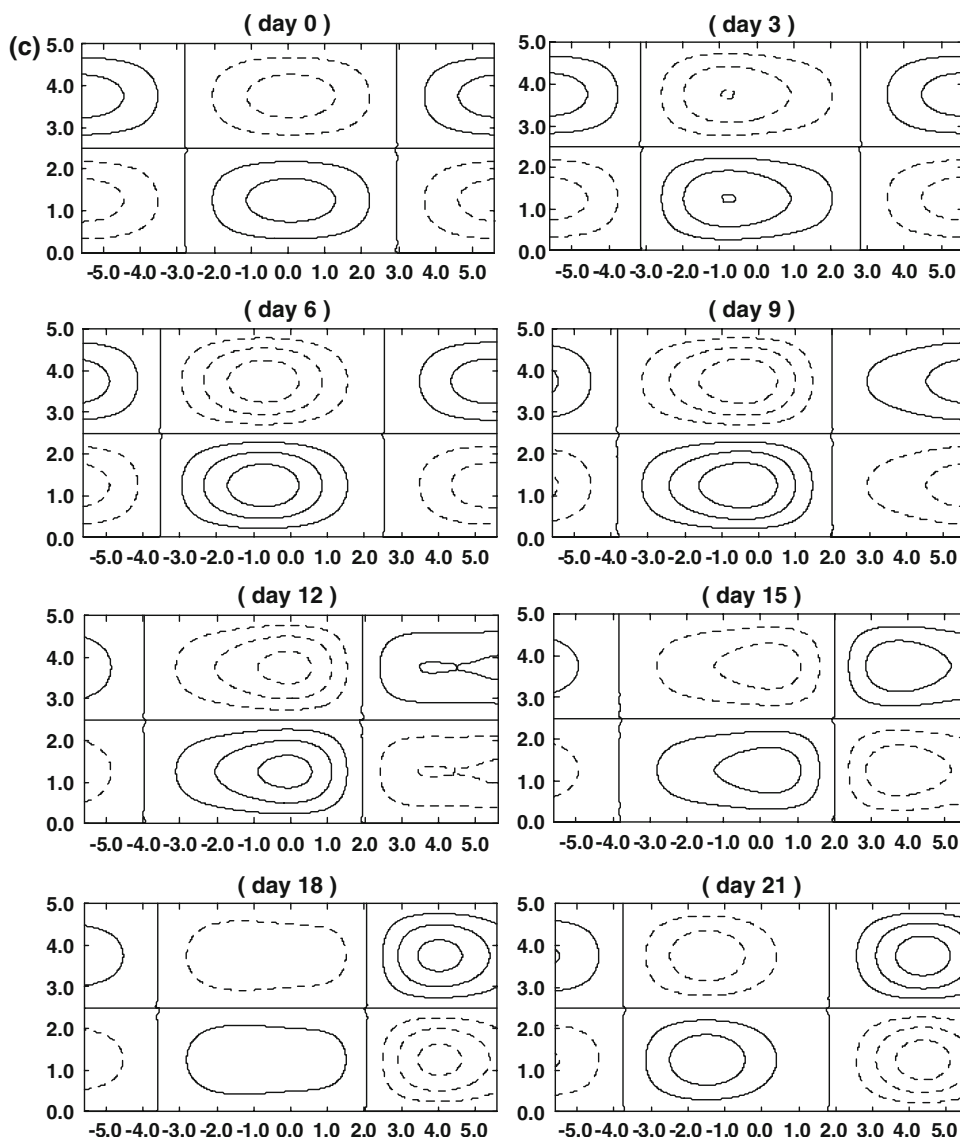
values of the NAO anomaly, jet shift, the strength and spatial distribution of the Atlantic storm track (not shown). For example, in the presence of large-scale topography the inclusion of a northward shifting jet can enhance the zonal asymmetry of the eddy-driven NAO anomaly through intensifying the energy dispersion of Rossby waves toward the downstream (not shown). This result is new. In addition, it is also clear that during the decaying phase of the NAO+ event the downstream energy dispersion of Rossby waves is enhanced in the presence of a topographic wave anomaly when the prior Atlantic jet undergoes a localized northward shift.

Thus, the isolated structure and zonal asymmetry of the eddy-driven NAO anomaly are not only dominated by the strength and longitudinal distribution of the preexisting synoptic eddies and the initial value of the

NAO anomaly, but also by the topographic height (the strength of topographic wave anomaly) and the jet shift. It is, however, likely that the initial value of the NAO anomaly and the topographic height (the strength of topographic wave anomaly) are two more important factors for the zonal asymmetry of the NAO anomaly than the zonal localization of the preexisting storm track.

6 Occurrence of European blocking events and its link with positive-phase NAO events

Although a linkage between European blocking events and the positive phase of the NAO event has been theoretically investigated by Luo et al. (2007a), a precise
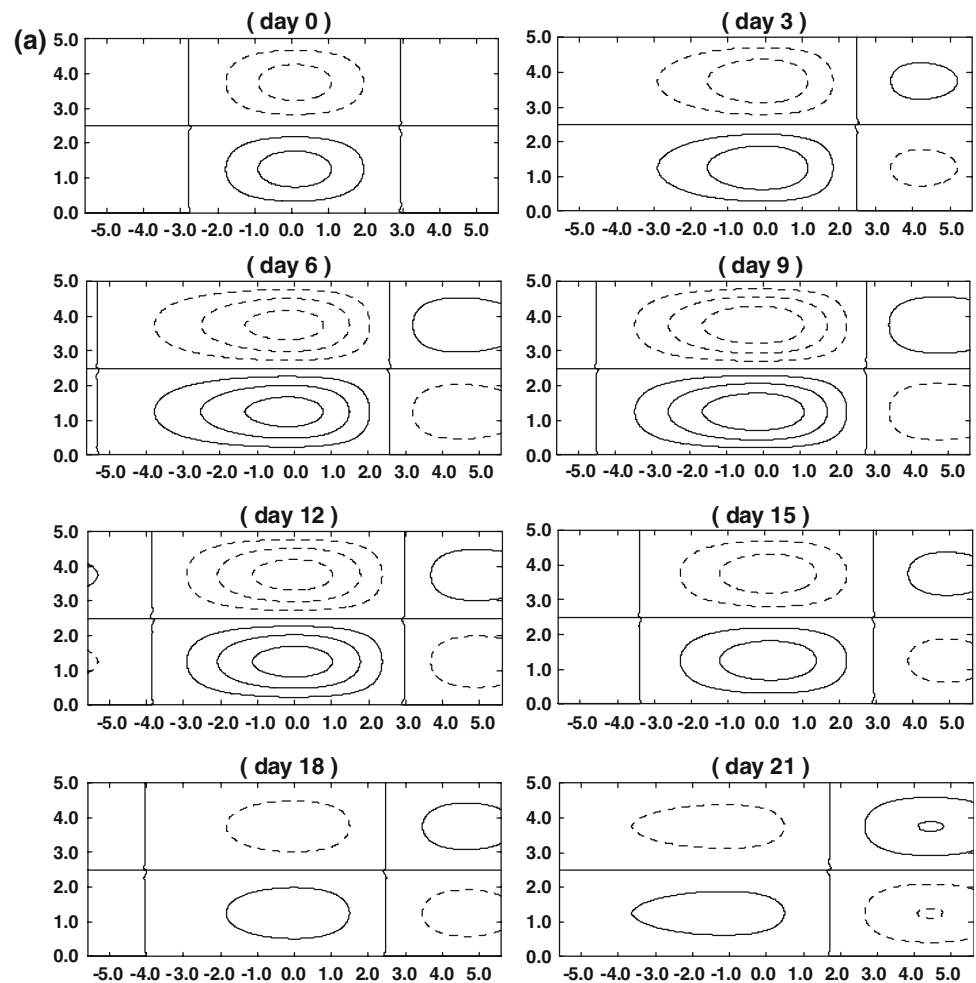
relationship of the onset of blocking events downstream of the Atlantic basin with the prior Atlantic jet, the initial value of the NAO and the longitudinal distribution of the Atlantic storm track is not examined in detail. In particular, the cause of why the positive phase of the NAO does not always correspond to the generation of European blocking is not identified previously. In this section, we will investigate what factors affect the occurrence of blocking events over the Europe region during the positive phase of the NAO using an extended nonlinear NAO model derived above.

6.1 Effect of the meridional shift of an Atlantic jet

For the initial value of $B(x, 0) = 0.4$, Fig. 10 shows the planetary-scale field (ψ_P) of a NAO$^+$ life cycle in the presence of a topographic wave anomaly under the forcing of almost uniform synoptic-scale eddies ($\mu = 0.12$) in a jet without ($\alpha_{S0} = 0$) and with ($\alpha_{S0} = -0.15$) a meridional shift.

It is seen that when the amplitude of the initial NAO anomaly is uniform, a NAO$^+$ event can be produced over the Atlantic basin, and two blocking events occur simultaneously in the downstream region (Europe continent) of the Atlantic basin during the period from day 18 to day 48 through the decaying of the NAO$^+$ event, in which the first blocking event is relatively short-lived. However, the two blocking events are combined into a long-lived, strong blocking event when the Atlantic jet undergoes a northward shift (Fig. 10b). The enhancement of the European blocking may be attributed to the prominent enhancement of the energy dispersion of Rossby waves toward downstream during the decaying process of the NAO$^+$ event as the Atlantic jet exhibits a northward shift. This result is consistent with the finding of Luo et al. (2008b), who noted that the northward shift of the Atlantic jet favors the occurrence of strong European blockings. Of course, the position of the maximum shift of a jet can also affect the blocking action in the Europe sector (not shown). In addition, we can also see that when the Atlantic jet with

Fig. 8 continued
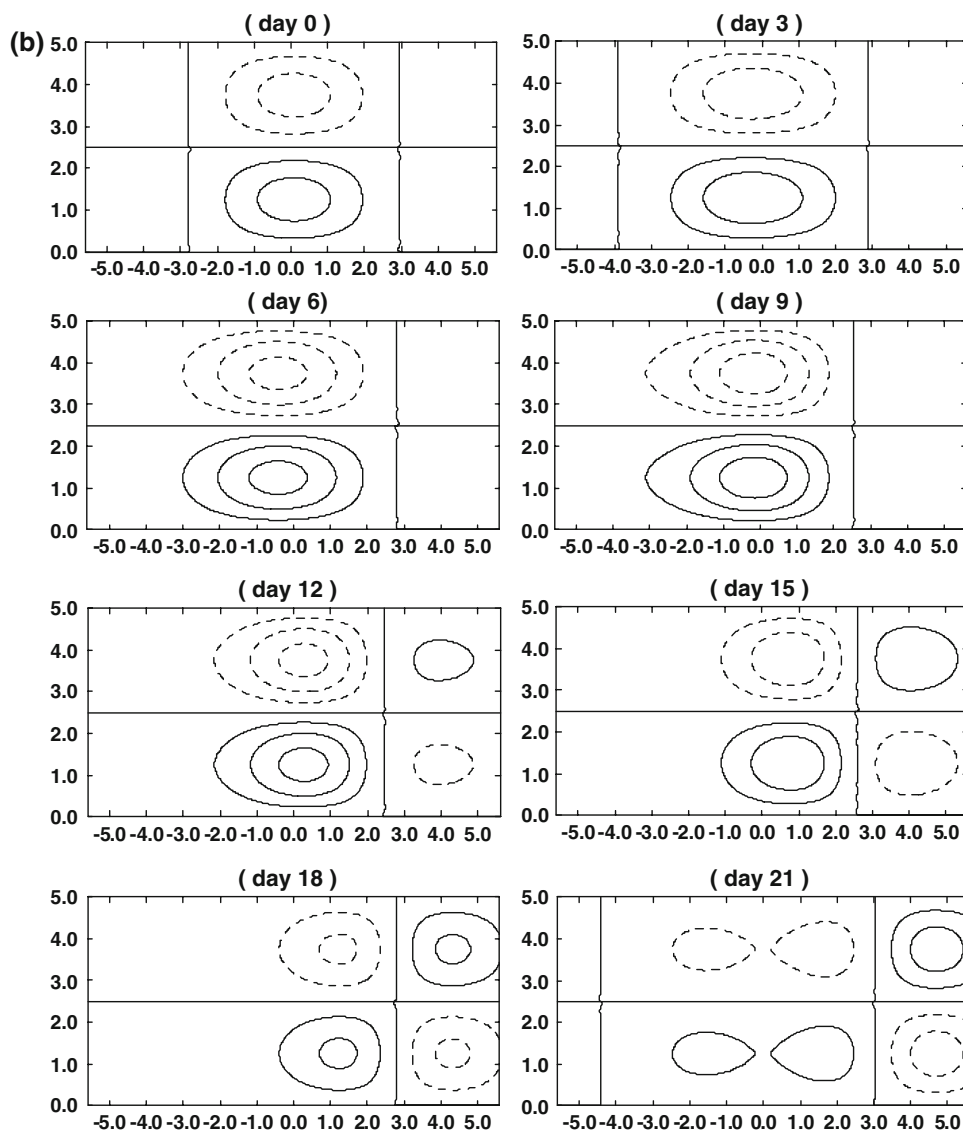
no shift is stronger, the European blocking will be suppressed (not shown).

6.2 Effect of the strength and zonal localization of the preexisting Atlantic storm track

For the same parameters as in Fig. 10b, Fig. 11 shows the planetary-scale field of a NAO$^+$ life cycle for the forcing of more zonally localized synoptic-scale eddies ($\mu = 4.8$). It is seen that during the life cycle of NAO$^+$ events the strength, lifetime and spatial structure of European blocking events are influenced by the zonal localization of preexisting synoptic-scale eddies. When the preexisting eddies in the Atlantic basin are more zonally localized, the intensity (duration) of the European blocking event

becomes weaker (shorter). Of course, the blocking activity over the European continent is also influenced by the strength of preexisting synoptic eddies (not shown). It is easily found that the Europe blocking becomes more robust and persistent if preexisting synoptic-scale eddies are stronger (not shown). Moreover, a dipole block structure can also appear over the Europe continent during the whole period from the onset to the decay. Thus, it is possible that the strength, lifetime and structure of European blocking events are influenced by the strength and longitudinal distribution of the Atlantic storm track during the NAO$^+$ life cycle. Thus, a change in the Atlantic storm track in position and strength can affect the activity of European blocking. This result is new compared to the finding in Luo et al. (2008b).

Fig. 8 continued
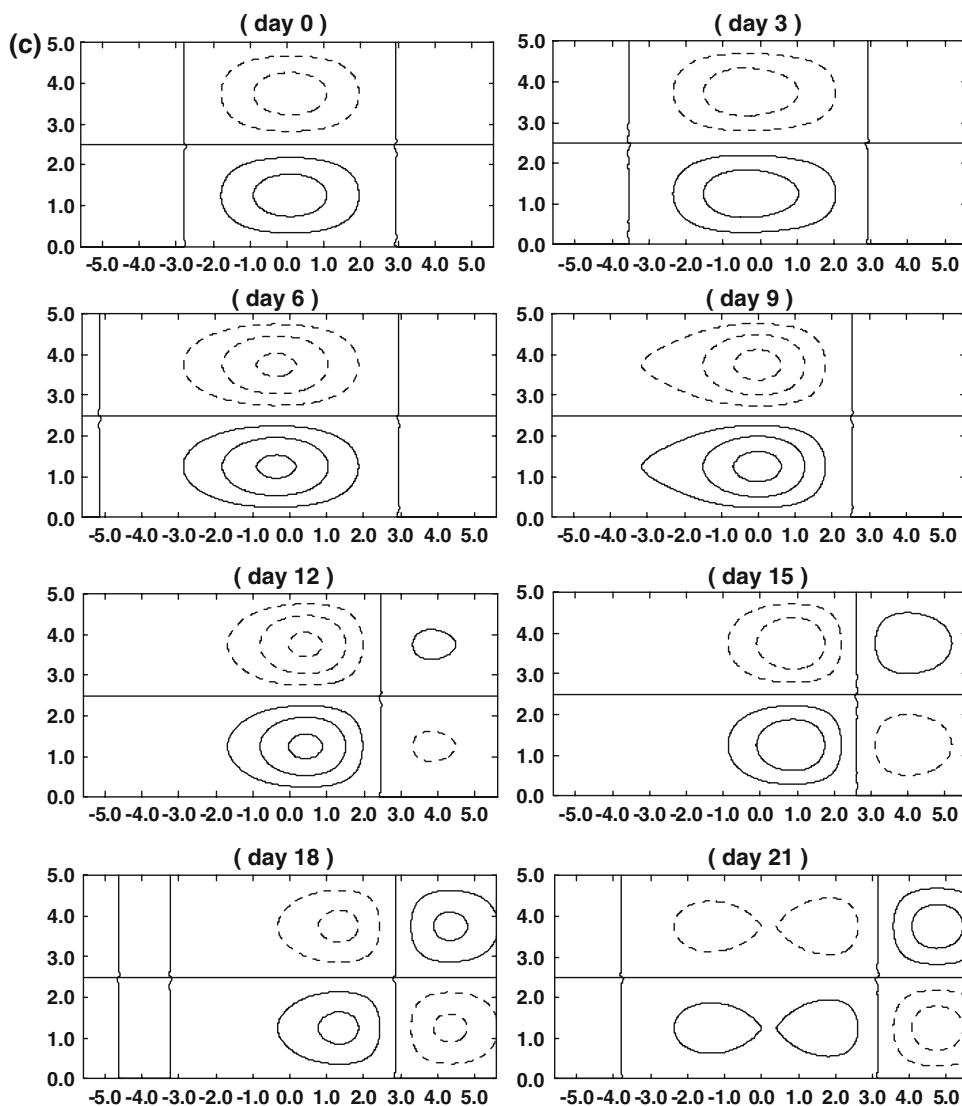
## 6.3 Effect of the initial value of the NAO$^+$ anomaly

For the initial value of $B(x,0) = 0.4e^{-0.08x^2}$ and for the same parameters as in Fig. 10b, the planetary-scale field of the NAO$^+$ life cycle is shown in Fig. 12 for $\mu = 0.12$ and $\mu = 4.8$, respectively.

It is seen from a comparison with Fig. 10b that when the initial value of the NAO$^+$ anomaly is zonally localized, the resulting blocking event in the Europe sector becomes rather weak relative to in Fig. 10b under the same parameter condition and its amplitude exhibits a distinct two peaks during its life cycle similar to a bimodal behavior observed by Cerlini et al. (1999). If the preexisting synoptic-scale eddies are more zonally localized, the excited European blocking is evidently weakened and its

life period is significantly shortened (Fig. 12b). This can be evidently seen from a comparison with Fig. 11. However, no blocking event is observed in the Europe sector if the northward shift of the prior Atlantic jet is relatively weak (not shown). Thus, the initial value of the NAO$^+$ anomaly in the Atlantic basin can exert an important influence on the occurrence of blocking events over the Europe region during the life cycle of NAO$^+$ events, but its influencing extent depends strongly on the meridional shift of the prior Atlantic jet.

The above discussions indicate that the variability of blocking events in location, duration and intensity over the European continent is not only dominated by the longitudinal distributions of both the preexisting synoptic-scale eddies and initial value of the NAO$^+$ anomaly, but also by

Fig. 9 Anomaly field ψ_{NAOA} of the eddy-driven positive-phase NAO life cycle in a northward shifting jet ($\alpha_{S0} = -0.15$) for the initial value of $B(x,0) = 0.4e^{-0.08x^2}$ under the forcing of synoptic-scale eddies with different zonal distributions (CI=0.2): **a** $\mu = 0.12$, **b** $\mu = 2.4$ and **c** $\mu = 4.8$
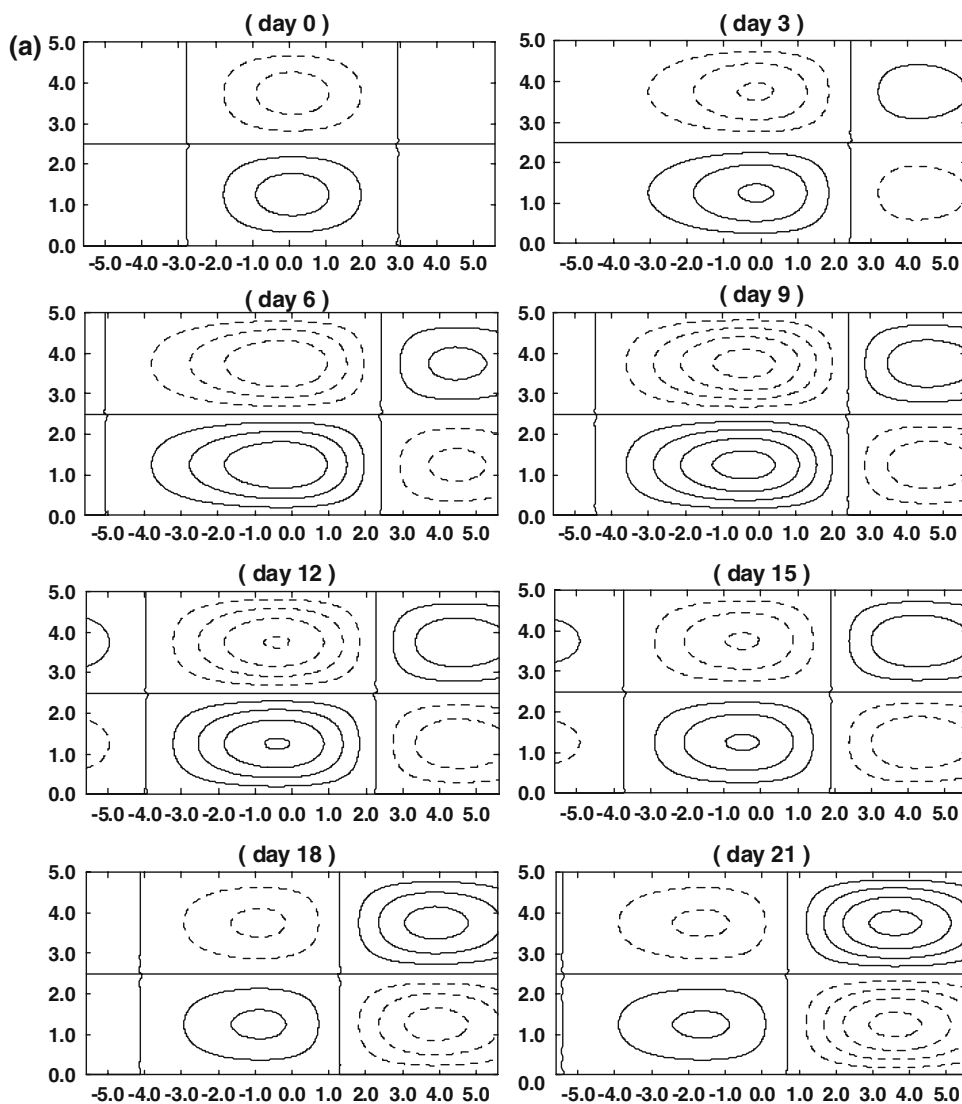

the variability in the prior Atlantic jet in position and strength. Thus, the variation of anyone in the three factors will result in the blocking variability over the European continent. This finding is new, which is not reported previously.

7 Jet structure and its local variability

To understand the local variability of the jet structure associated with the NAO, here we try to look at how the mean westerly wind responds to the NAO life cycle for its two phases. For the initial condition of $B(x,0) = 0.4e^{-0.08x^2}$ and for the same parameters as in Fig. 12b, $u_m(x, y, t)$ is shown in Fig. 13 during a NAO life cycle under the forcing of zonally localized synoptic-scale eddies ($\mu = 4.8$) in a symmetric jet for its two phases.

It is obvious that for the positive phase the zonal jet is enhanced in the higher latitudes and weakened in the lower latitudes (Fig. 13a), which is consistent with the jet distribution for the observed positive phase NAO (Fig. 1a). But for the negative phase the jet is strengthened in lower latitudes, but weakened in higher latitudes respectively (Fig. 13b), thus in agreement with the jet distribution of the observed negative phase NAO (Fig. 1a). This indicates that the jet structures obtained in our model are basically consistent with observed jet structures of the NAO for its two phases (Fig. 1a). If a subtropical jet exists as observed in the NH, then it is inevitable that the double jet structure appears for the positive phase which is directly related to the separation between the eddy-driven Atlantic jet and the subtropical jet whereas a single jet structure clearly appears for the negative phase. On the other hand this jet structure is found to exhibit a distinct low-frequency variation with a

Fig. 9 continued
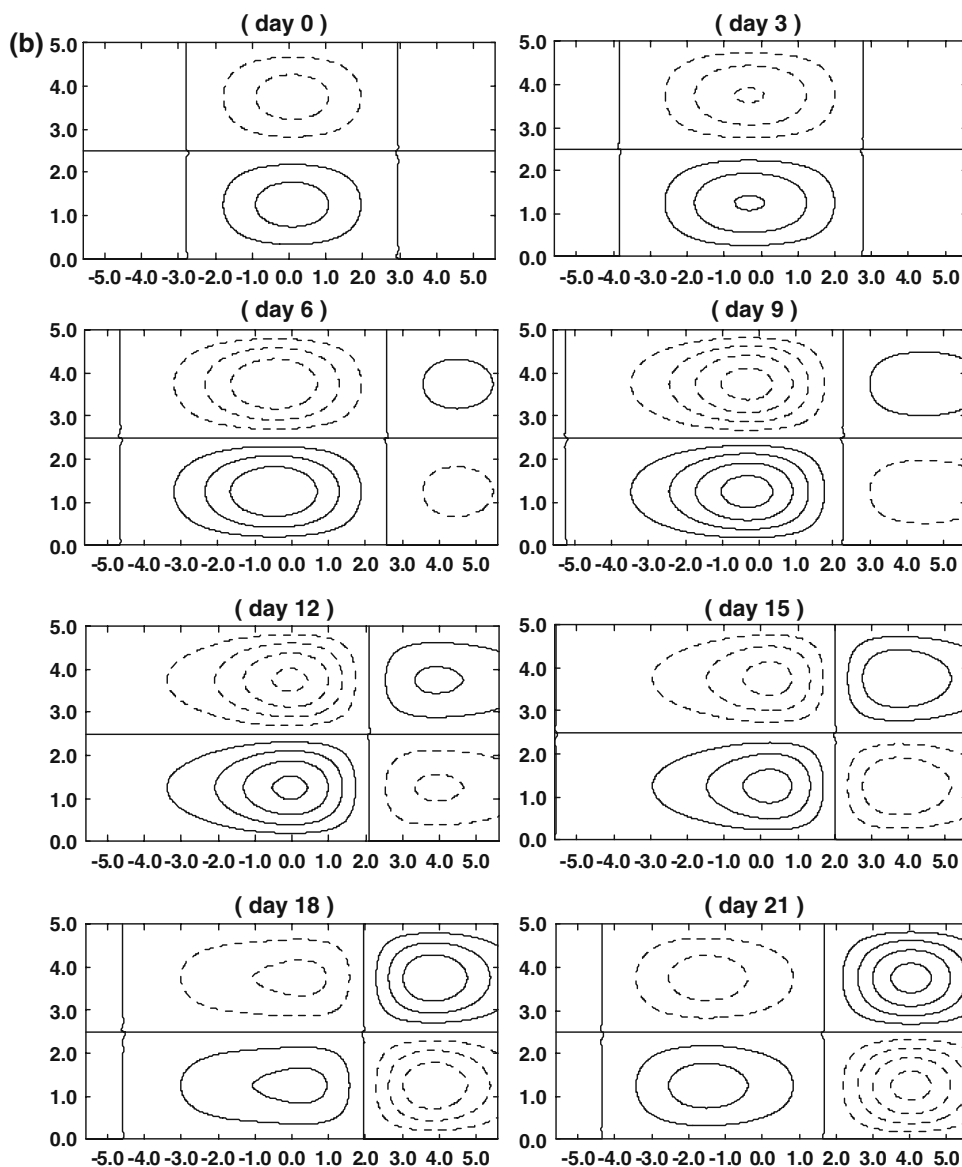
period identical to the timescale of the eddy-driven NAO anomaly because the NAO amplitude is involved in u_m. As has mentioned by Luo et al. (2007b), the variability in jet structure is mainly dominated by the eddy-driven NAO anomaly itself and its interaction with topographic stationary wave, rather than directly by the synoptic-scale eddies. It is also clear that when the eddy-driven NAO anomaly is zonally isolated, the mean westerly wind u_m is inevitably zonally isolated. This finding is consistent with the observation shown in Fig. 1 for two phases of the NAO. When the prior Atlantic jet undergoes a meridional shift, the variability in jet strength and position is more distinct (not shown). Although the spatial-temporal evolution of the zonal jet during the NAO life cycle gained in a theoretical model is highly idealized, it bears a striking resemblance to

the observed variability in jet structure over the Atlantic basin during the NAO episode.

In the real atmosphere, because the latitudinal shift of the westerly jet is mainly confined in the Atlantic basin (Lee and Kim 2003), the initial NAO anomaly excited by the interaction between the zonal jet and topographic stationary wave is in principle zonally isolated. On the other hand, because the Atlantic storm track is mainly localized in the upstream side of the Atlantic basin, the occurrence of zonally isolated and asymmetric NAO patterns is an inevitable result of the interaction between the localized planetary-scale wave and localized synoptic-scale eddies in the Atlantic sector, thus inevitably resulting in a localized variability in the jet structure associated with the NAO.

Fig. 9 continued
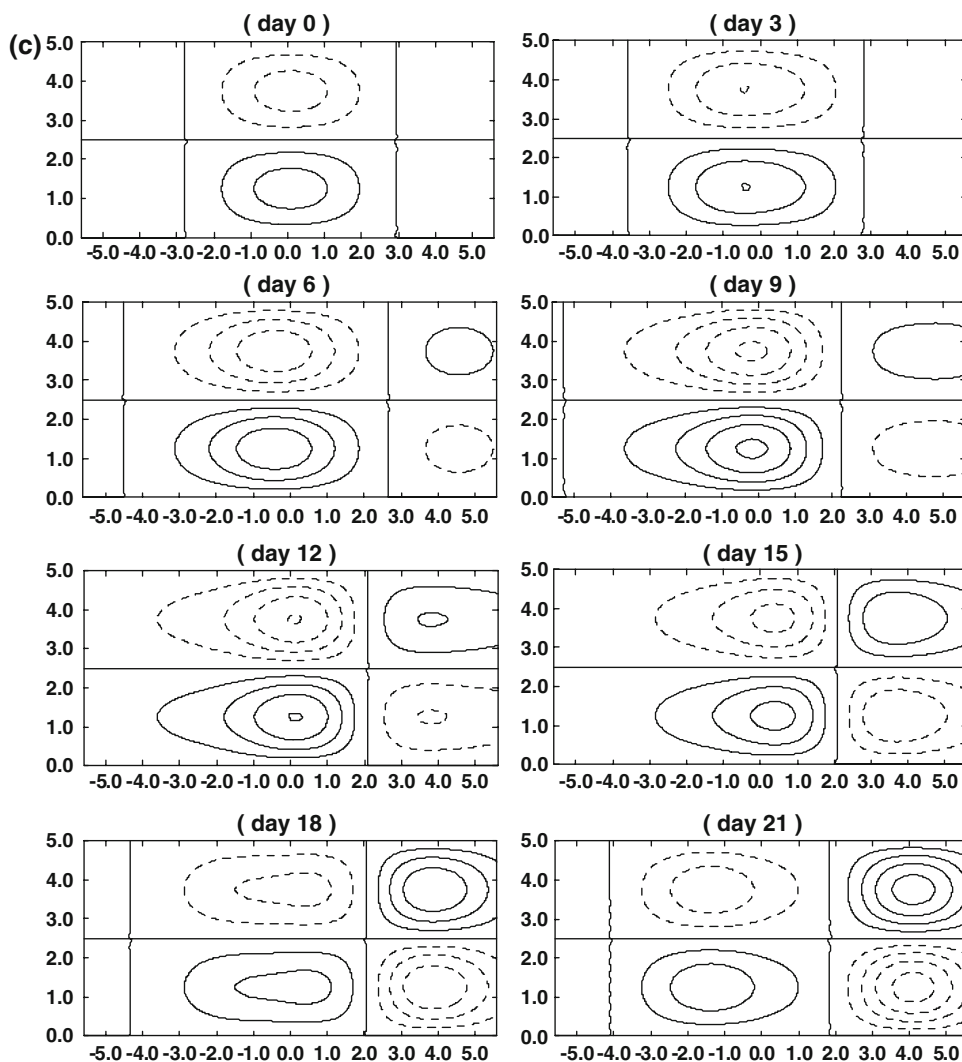
8 Conclusion and discussions

In this paper, we have extended the weakly nonlinear NAO model established by Luo et al. (2008b) to identify what factors affect the zonal structure (isolated structure and zonal asymmetry) of the observed NAO pattern. It is found that the zonal structure of eddy-driven NAO patterns does not only depend upon the strength and longitudinal distribution of the Atlantic storm track and the initial condition of the NAO anomaly associated with the latitudinal shift of a preexisting Atlantic jet, but also on the topographic height and the strength of the jet shift. When the Atlantic storm track is more zonally localized, more energy of Rossby waves can be accumulated in a narrow region, thus resulting in a more zonally localized dipole mode resembling an observed isolated NAO anomaly, albeit the initial NAO anomaly may be zonally uniform. However, if the initial NAO anomaly excited by the interaction between a

localized shifting jet and a topographic wave ridge over the Atlantic sector is zonally localized, a robust isolated NAO pattern can be formed and simultaneously exhibits a strong zonal asymmetry even though the Atlantic storm track may be almost zonally uniform. Nevertheless, it is difficult to observe robust zonally isolated NAO patterns if both the Atlantic storm track and the initial NAO anomaly are almost zonally uniform. On the other hand, it is found that although the zonal localization of the Atlantic storm track is important for the zonal structure of the NAO anomaly, the initial condition of the NAO associated with the localized shift of a prior Atlantic jet is likely to be more important for the zonal asymmetry of the eddy-driven NAO anomaly. The presence of large-scale topography tends to enhance the zonal asymmetry of the NAO anomaly even though affected by the initial value of the NAO anomaly, the strength and longitudinal distribution of the preexisting synoptic eddies and the jet shift.

Fig. 10 Planetary-scale field (ψ_P) of a NAO$^+$ life cycle in the presence of a topographic wave anomaly for the initial value of $B(x, 0) = 0.4$ under the forcing of almost uniform synoptic-scale eddies ($\mu = 0.12$) in a background jet (CI = 0.15): **a** without the meridional shift ($\alpha_{S0} = 0$) and **b** with ($\alpha_{S0} = -0.15$) the meridional shift
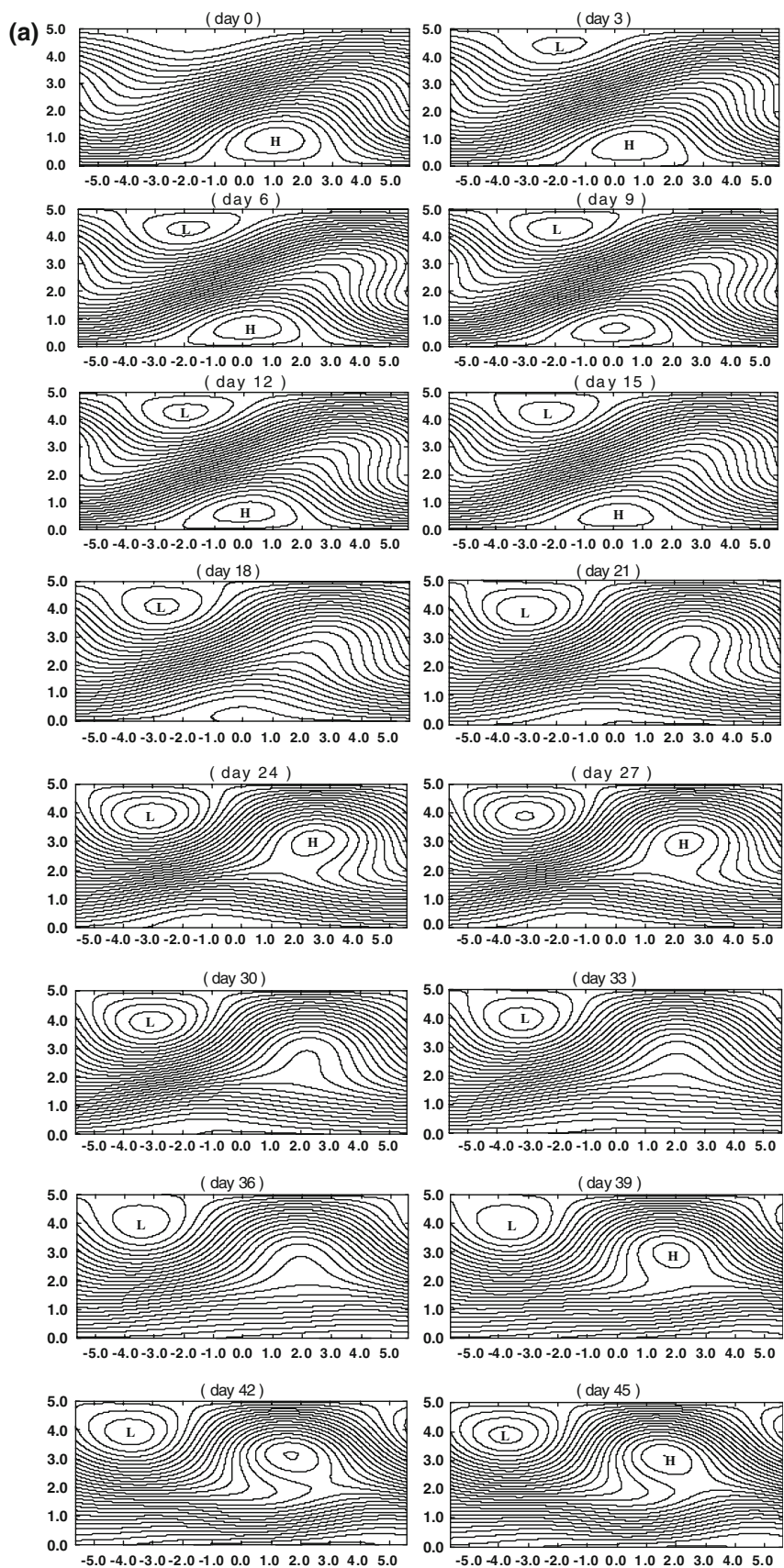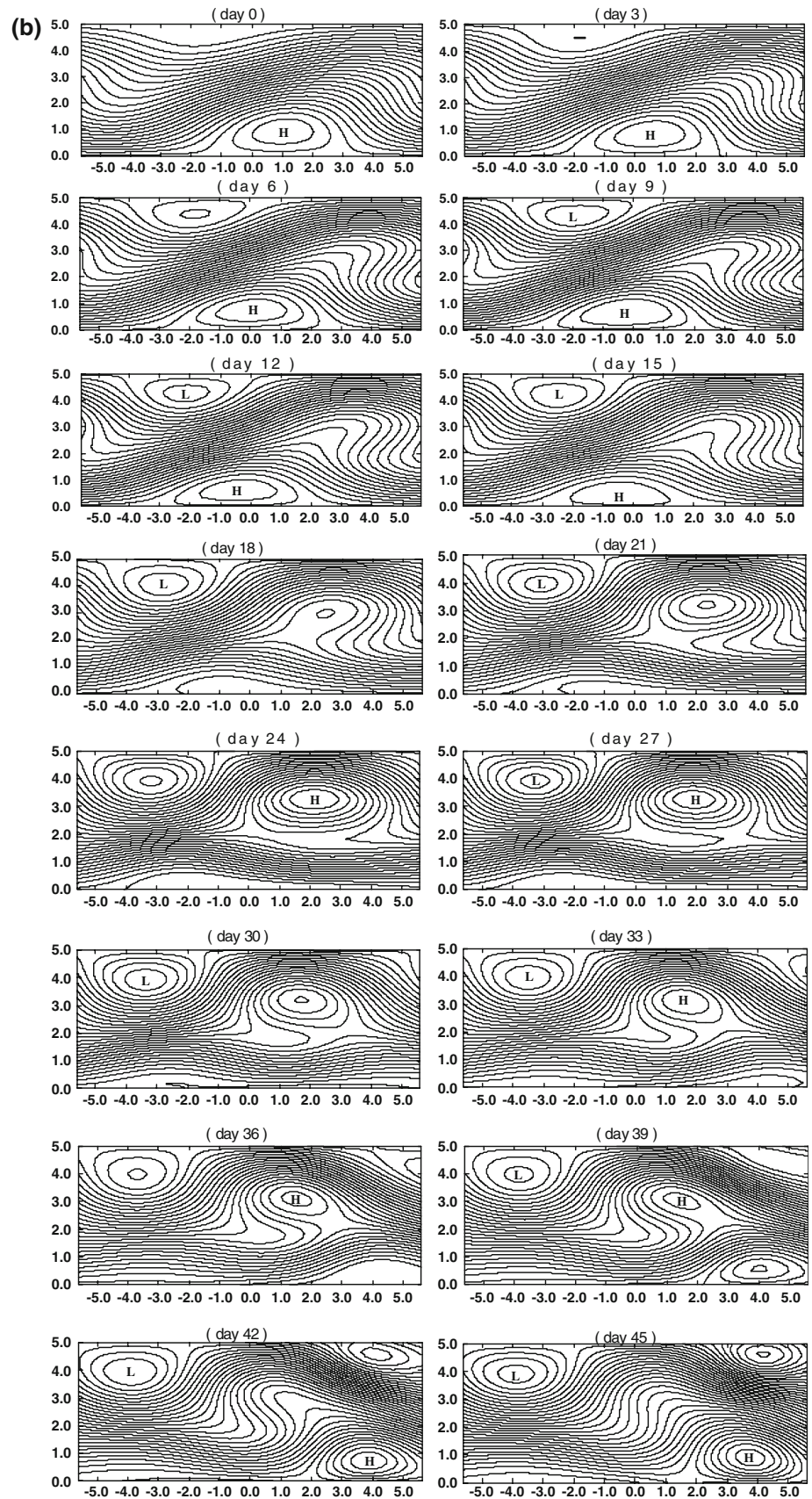
Fig. 10 continued

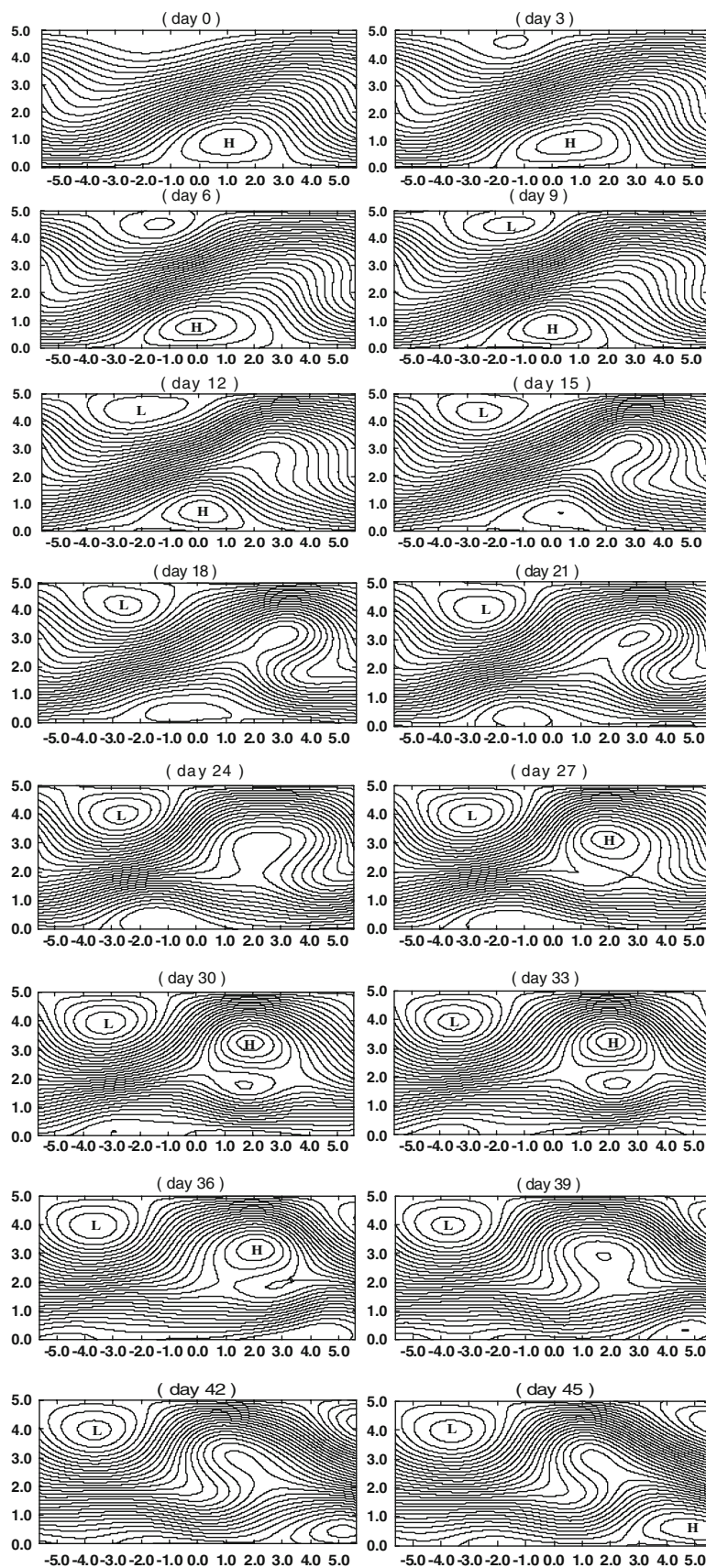**Fig. 11** As Fig. 10b but for the forcing of more zonally localized synoptic- scale eddies ($\mu = 4.8$)

Fig. 12 As Fig. 10b but for the initial value of $B(x,0) = 0.4e^{-0.08x^2}$ and for the forcing of synoptic-scale eddies with two different zonal distributions: **a** $\mu = 0.12$ and **b** $\mu = 4.8$
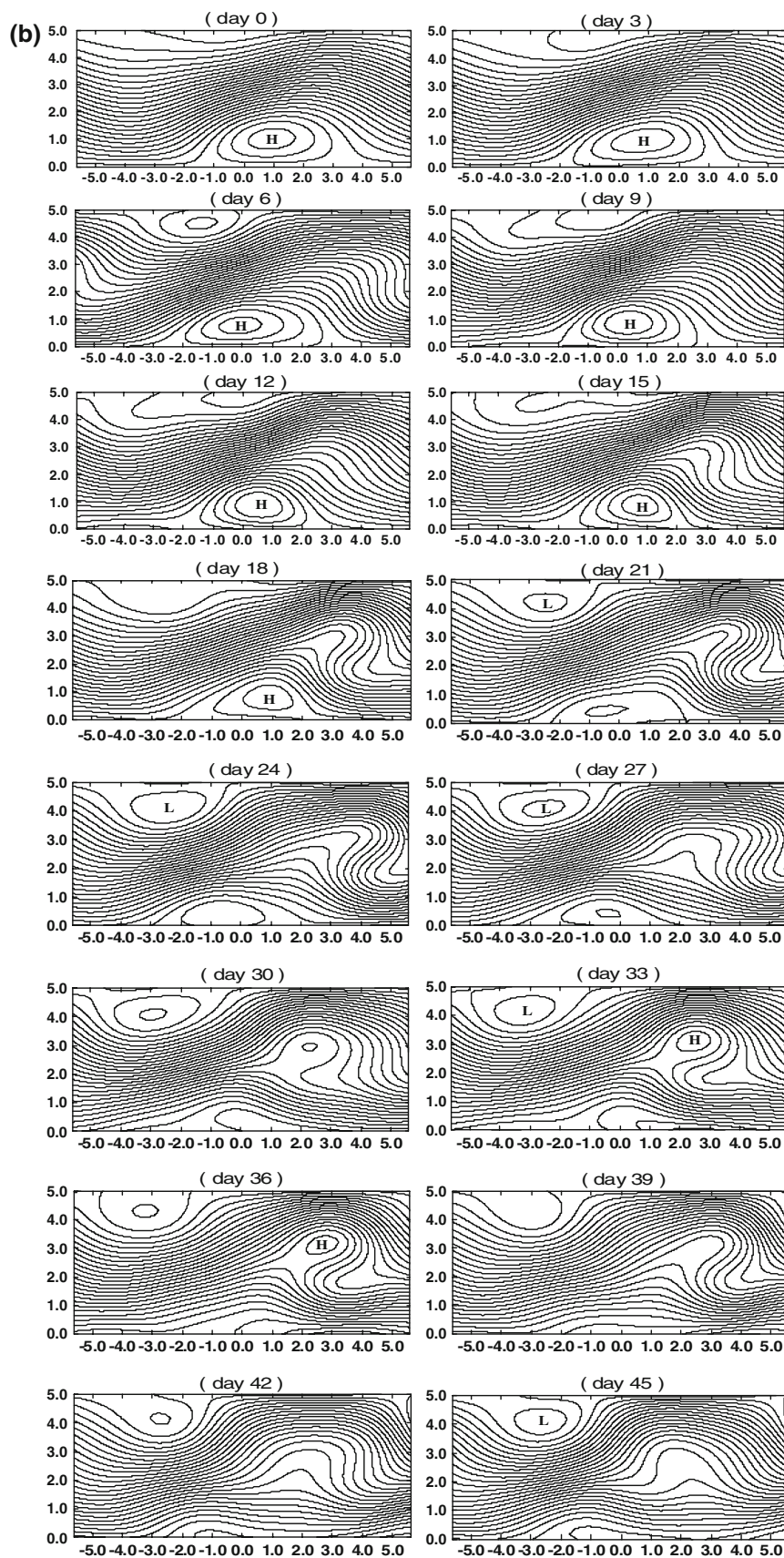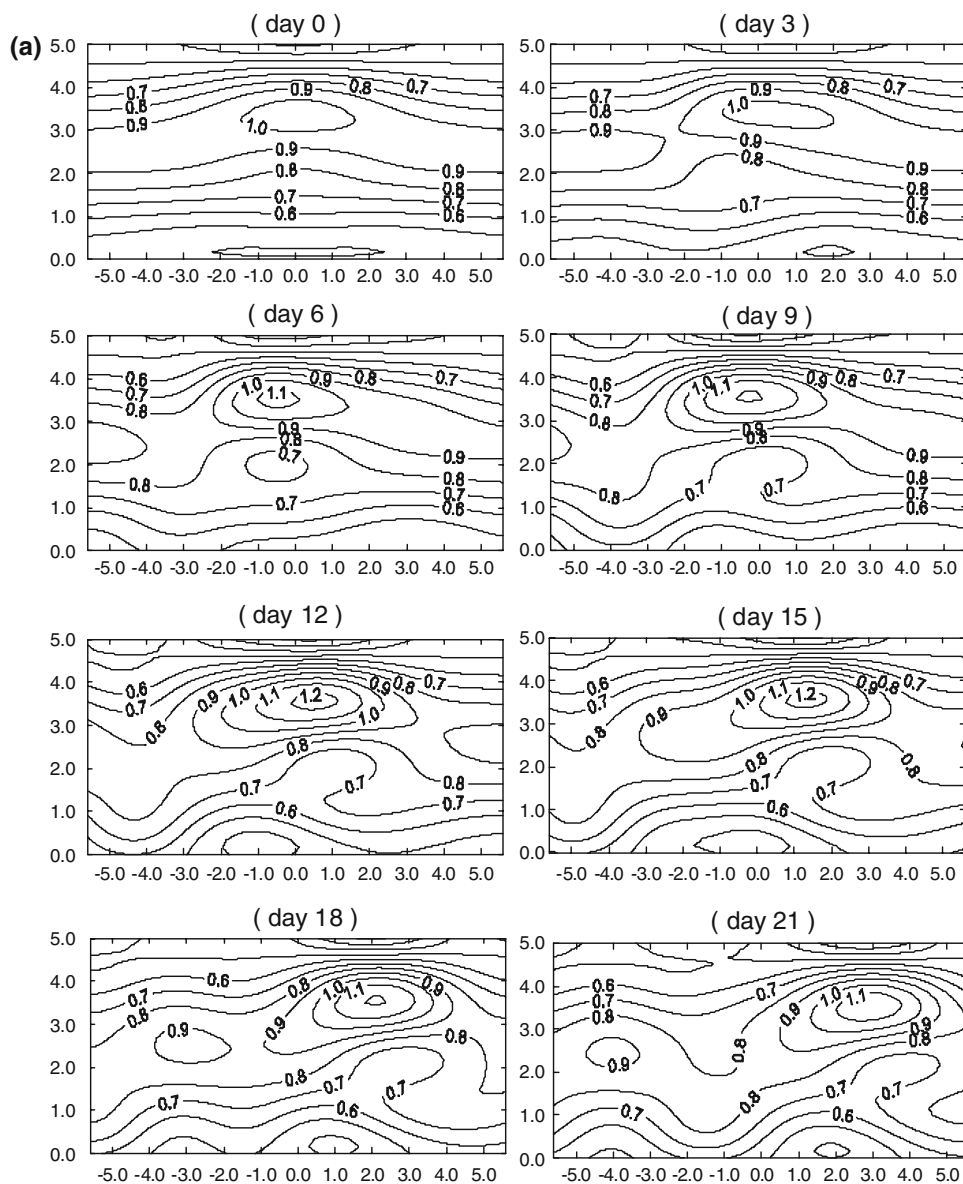
Fig. 12 continued

(b)
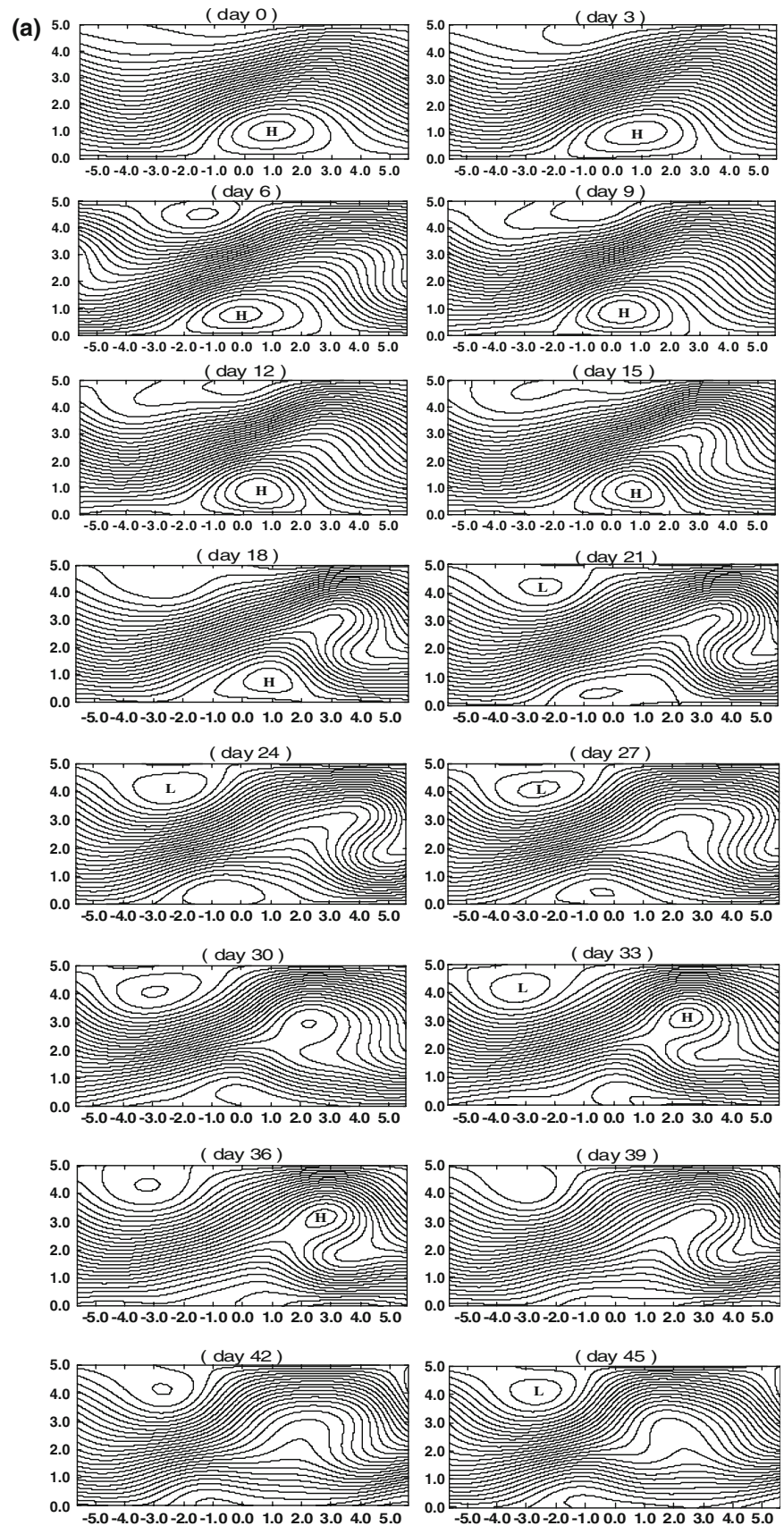
Fig. 13 Instantaneous horizontal distribution of $u_m(x, y, t)$ during the NAO life cycle in a symmetric jet for the initial condition of $B(x, 0) = 0.4e^{-0.08x^2}$ under the forcing of zonally localized synoptic-scale eddies ($\mu = 4.8$) for the same parameters as in Fig. 12b: **a** positive phase and **b** negative phase

Furthermore, it is found that the variability in blocking frequency, persistence and intensity over the European continent depends, to large extent, upon the latitudinal shift of the prior Atlantic jet, the strength and longitudinal distribution of the Atlantic storm track prior to the NAO and the initial condition of the NAO anomaly. This may explain why there is not the one-to-one correspondence between the positive phase NAO event and the occurrence of the European blocking event. During the decaying of the positive phase NAO, blocking events occurred over the European continent can sometimes exhibit two peaks during the lifecycle of blocking.

It must be pointed out that the localized latitudinal shift of a prior Atlantic jet is pre-specified in this paper. What dynamical process drives such a localized meridional shift of the prior Atlantic jet and the zonal variability of the prior Atlantic storm track is not clearly identified in this paper. In the future task, we will use the numerical model to detect what factors can control the latitudinal shift of the prior Atlantic jet and longitudinal distribution of the Atlantic storm track prior to the NAO. It can help us improve our understanding of the phase transition of the NAO and its link with the local and global warming.

Fig. 13 continued
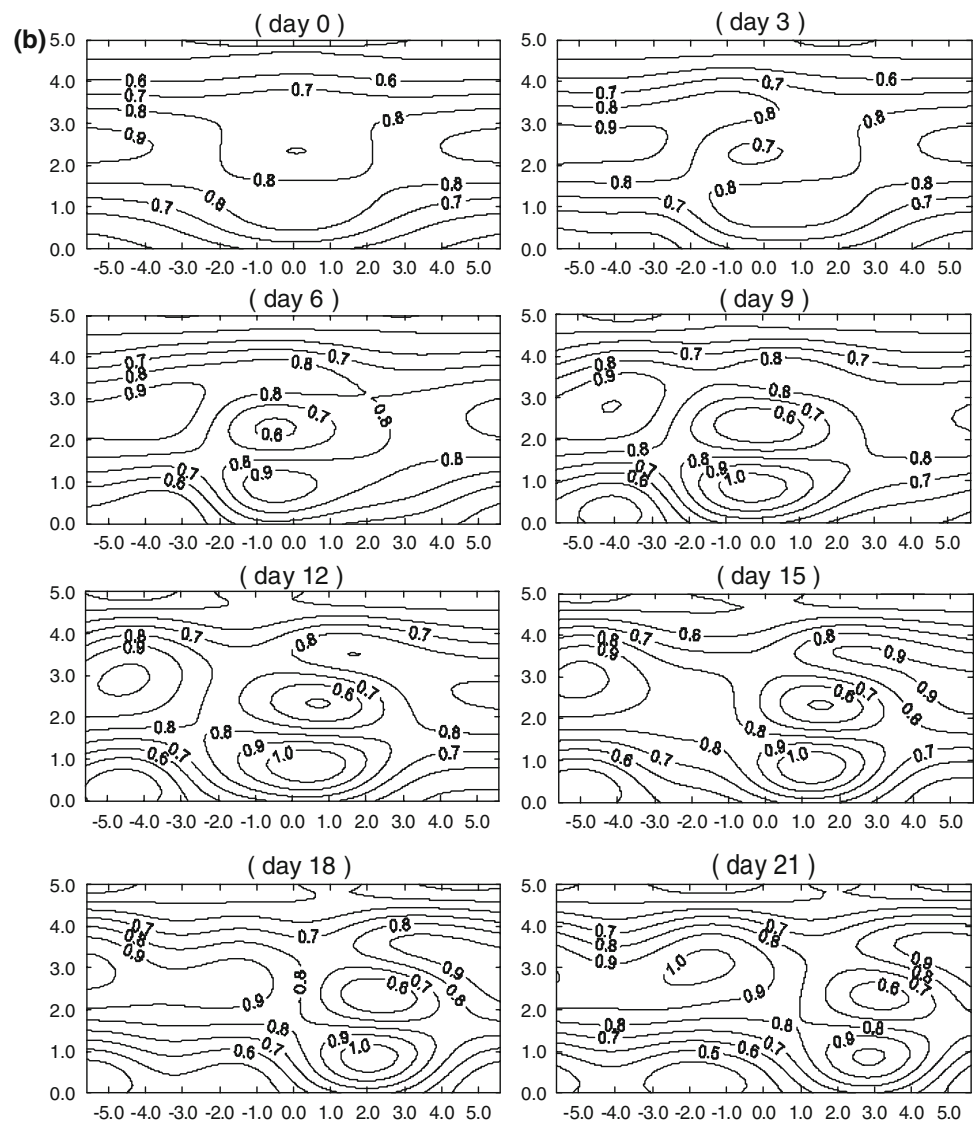
References

Benedict JJ, Lee S, Feldstein SB (2004) Synoptic view of the North Atlantic Oscillation. J Atmos Sci 61:121–144

Cash BA, Kushner PJ, Vallis GK (2002) The structure and composition of the annular modes in an aquaplanet general circulation model. J Atmos Sci 59:3399–3414

Cash BA, Kushner PJ, Vallis GK (2005) Zonal asymmetries, teleconnections and annular patterns in a GCM. J Atmos Sci 62:207–219

Cerlini PB, Corti S, Tibaldi S (1999) An intercomparison between low-frequency variability indices. Tellus 51A:773–789

DeWeaver E, Nigam S (2000) Do stationary wave drive the zonal-mean jet anomalies of the Northern winter? J Clim 13:2160–2176

Eichelberger SJ, Hartmann DL (2007) Zonal jet structure and the leading mode of variability. J Clim 20:5149–5163

Feldstein SB (2003) The dynamics of NAO teleconnection pattern growth and decay. Q J R Meteor Soc 127:901–924

Feldstein SB, Franzke C (2006) Are the North Atlantic Oscillation and Northern annular mode distinguishable? J Atmos Sci 63:1915–2930

Feliks Y, Ghil M, Simonnet E (2004) Low-frequency variability in the midlatitude atmosphere induced by an oceanic thermal front. J Atmos Sci 61:961–981

Franzke C, Lee S, Feldstein SB (2004) Is the North Atlantic Oscillation a breaking wave? J Atmos Sci 61:145–160

Gerber EP, Vallis GK (2005) A stochastic model for the spatial structure of annular pattern of variability and the North Atlantic Oscillation. J Clim 18:2102–2118

Hurrell JW (1995) Decadal trends in the North Atlantic oscillation: regional temperatures and precipitation. Science 269:676–679

Lee S, Kim H (2003) The dynamical relationship between subtropical and eddy-driven jets. J Atmos Sci 60:1490–1503

Limpasuvan V, Hartmann DL (1999) Eddies and the annular modes of climate variability. Geophys Res Lett 26:3133–3136

Löptien U, Ruprecht E (2005) Effect of synoptic systems on the variability of the North Atlantic Oscillations. Mon Wea Rev 133:2894–2904

Luo D, Lupo A, Wan H (2007a) Dynamics of eddy-driven low frequency dipole modes. Part I: a simple model of North Atlantic Oscillations. J Atmos Sci 64:3–38

Luo D, Gong T, Diao Y (2007b) Dynamics of eddy-driven low frequency dipole modes. Part III: meridional displacement of westerly jet anomalies during two phases of NAO. J Atmos Sci 64:3232–3248

Luo D, Gong T, Diao Y (2008a) Dynamics of eddy-driven low frequency dipole modes. Part IV: planetary and synoptic wave breaking processes during the NAO life cycle. J Atmos Sci 65:737–765

Luo D, Gong T, Zhong L (2008b) Dynamical relationship between the phase of North Atlantic Oscillations and the meridional excursion of a preexisting jet: an analytical study. J Atmos Sci 65:1838–1858

Mak M (2002) Wave-packet resonance: instability of a localized barotropic jet. J Atmos Sci 59:823–836

Pedlosky J (1987) Geophysical fluid dynamics. Springer, Heidelberg

Pierrehumbert RT (1984) Local and global baroclinic instability of zonally varying flow. J Atmos Sci 41:2141–2162

Scherrer SC, Maspoli MC, Schwierz C, Appenzeller C (2006) Two-dimensional indices of atmospheric blocking and their statistical relationship with winter climate patterns in the Euro-Atlantic region. Int J Climatol 26:233–249

Swanson KL (2001) Oscillatory instabilities to zonally varying barotropic flows. J Atmos Sci 58:3135–3147

Thompson DWJ, Wallace JM (1998) The Arctic Oscillation signature in wintertime geopotential height and temperature fields. Geophys Res Lett 25:1297–1300

Thompson DWJ, Wallace JM, Hegerl GC (2000) Annular modes in the extratropical circulation. Part II: trends. J Clim 13:1018–1036

Thorncroft CD, Hoskins BJ, McIntyre ME (1993) Two paradigms of baroclinic wave life-cycle behavior. Q J R Meteor Soc 119:17–55

Vallis GK, Gerber EP (2008) Local and Hemispheric dynamics of the North Atlantic Oscillation, Annular patterns, and the zonal index. Dyn Atmos Oceans 44:184–280

Vallis GK, Gerber EP, Kushner PJ, Cash BA (2004) A mechanism and simple dynamical model of the North Atlantic Oscillation and annular modes. J Atmos Sci 61:264–280

Wallace JM (2000) North Atlantic Oscillation/Annular mode: two paradigms-one phenomenon. Q J R Meteoro Soc 126:791–805

Whitaker JS, Dole RM (1995) Organization of storm tracks in zonally varying flows. J Atmos Sci 52:1178–1191